Performance Analysis of Composite Insulators up to 1200 kV ac using Electric Field Calculations

by

Tanushri Doshi

A Thesis Presented in Partial Fulfillment
of the requirements for the Degree
Master of Science

Approved November 2010 by the
Graduate Supervisory Committee:

Ravi Gorur, Chair
Richard Farmer
Vijay Vittal

ARIZONA STATE UNIVERSITY

December 2010

ABSTRACT

This research work illustrates the use of software packages based on the concept of numerical analysis technique to evaluate the electric field and voltage distribution along composite insulators for system voltages ranging from 138 kV up to 1200 kV ac. A part of the calculations was made using the 3D software package, COULOMB 8.0, based on the concept of Boundary Element Method (BEM). The electric field was calculated under dry and wet conditions. Composite insulators experience more electrical stress when compared to porcelain and are also more prone to damage caused by corona activity. The work presented here investigates the effect of corona rings of specific dimensions and bundled conductors on the electric field along composite insulators. Inappropriate placement or dimensions of corona rings could enhance the electric field instead of mitigating it. Corona ring optimization for a 1000 kV composite insulator was performed by changing parameters of the ring, such as the diameter of the ring, thickness of the ring tube and the projection of the ring from the high voltage energized end fitting. Grading rings were designed for Ultra High Voltage (UHV) systems that use two units of composite insulators in parallel. The insulation distance, which bears 50% of the total applied voltage, is raised by 61% with the grading ring installed, when compared to the distance without the grading ring. In other words, the electric field and voltage distribution was found to be more linear with the application of grading rings.

The second part of this project was carried out using the EPRI designed software EPIC. This is based on the concept of Charge Simulation method (CSM). Comparisons were made between electric field magnitude along composite insulators used for suspension and dead end configuration for system voltages ranging from 138 kV to 500 kV. It was found that the dead end composite insulators experience significantly higher electrical stress when compared to their suspension counterpart. It was also concluded that this difference gets more prominent as the system voltage increases. A comparison made between electric field distribution along composite insulators used in single and double dead end structures suggested that the electric stress experienced by the single dead end composite insulators is relatively higher when compared to double dead end composite insulators.

To

my parents Seema Doshi and. Tarun Doshi

and brother Rishabh,

whose support is ever so precious

ACKNOWLEDGMENTS

I would like to sincerely thank my mentor and chair Dr. Ravi S. Gorur for his advice and continued support throughout my course. I greatly acknowledge and thank Mr. Jim Hunt from Salt River Project for providing me with an opportunity to work on this project. I express my gratitude towards Professor Farmer and Dr. Vijay Vittal for their time and consideration in being on my supervisory committee. I am also obliged to the faculty of the power systems group at Arizona State University for their guidance throughout my tenure here.

I would like to thank my parents and brother for their extended support without which this would not have been possible. I would also like to extend a special thanks to all my friends from Visvesvaraya National Institute of Technology and Arizona State University for always standing by me.

TABLE OF CONTENTS

Page

CHAPTER Page

LIST OF TABLES

LIST OF FIGURES

FIGURE Page

FIGURE Page

FIGURE Page

NOMENCLATURE

AC	Alternating Current
ACSR	Aluminium Conductor Steel Reinforced
BEM	Boundary Element Method
BIL	Basic Lightning Impulse Insulation Level
CSM	Charge Simulation Method
CDE	Compression Dead End Eye type
IES	Integrated Engineering Software
EFVD	Electric Field Voltage Distribution
EHV	Extra High Voltage
*EP*Link	Energized Link to Polymer
EPIC	EPRI Polymer Insulator Computation
EPRI	Electric Power Research Institute
FEM	Finite Element Method
GB	Giga Byte
*GP*Link	Grounded Link to Polymer
IEC	International Electrotechnical Commission
IEE	Institute of Electrical Engineers
IEEE	Institute of Electrical and Electronics Engineers
kV	Kilo Volts
RAM	Random Access Memory
SA	Socket to Eye
SAH	Structure Attachment Hardware
SAHD	Structure Attachment Horizontal Plate
SML	Specified Mechanical Load
Sqrt	Square Root
SRP	Salt River Project

SYC	Socket to Y Clevis
UHV	Ultra High Voltage

1. INTRODUCTION

1.1 Introduction to Outdoor Insulation

The generation and consumption of electric power are seldom in close vicinity. The bulk of electric power is transmitted through overhead lines from the generating sites to the distribution level. Most of these lines span over several thousands of kilometers. In order to minimize losses, power is transmitted at higher voltages in the order of several hundred kilovolts. The high voltage line conductor has to be physically attached to the tower support structure which is at ground potential. For the purpose of electrically isolating these line conductors from the support structure as well as providing mechanical support to them, insulators are used [1].

Most of the insulators are often under high electrical as well as mechanical stress. The ever increasing demand for electrical energy worldwide has lead to the use of even higher system voltages for power transmission. For instance, China has completed the construction of a 1000 kV ac system, India currently installed systems at 800 kV ac. Both India and China are planning to expand their systems to 1200 kV in the near future. Countries like The United States of America, Japan and Russia already have systems operating over 750 kV for many years [2]. Higher voltage rating puts the insulators under a huge amount of electrical stress. In addition to that, the high voltage insulators used in outdoor applications are degraded by various environmental factors including precipitation, winds, temperature variations and pollution. Under wet and polluted conditions, the electric field along their length gets intensified which might lead to flashover. Flashover of insulators in service could give way to interruptions in power supply which affects the reliability of these bulk systems. Also, interruptions could incur heavy monetary losses to many customers and industries. Therefore, insulation performance forms a small but extremely significant part of the whole picture. Research on its functionality and design is of utmost significance.

One of the major factors governing the electrical performance of composite insulators is the electric field distribution along their length. In order to understand and improve their performance, electric field analysis of high voltage composite insulators is necessary. Electric field distribution is affected by a variety of factors like the geometry of the insulator, tower configuration, the geometry of the attachment hardware, value of energized line voltage, presence of nearby

phases etc [3]. High electric field might lead to corona discharges on the surface of the composite insulator or the seals of the end fittings. There could be internal discharges along the fiberglass rod. In case of contamination, the property of hydrophobicity might be lost resulting in high surface leakage currents. In the work presented here, electric field calculations on composite insulators are shown for voltage ranging from 138 kV to 1200 kV ac. The effect of corona rings and bundled conductors on the electric field along composite insulators is analyzed. Composite insulators are known to be more prone to corona related damage when compared to porcelain [4]. Electric field analysis is carried out to determine the need for application of corona rings for different voltage levels.

The Electric Field and Voltage Distribution (EFVD) along composite insulators is more non-linear than porcelain insulators [5]. Corona ring installation not only mitigates the highest electric field but also shifts it away from the junction of the high voltage energized end fitting and the polymer material. Unfortunately, there are no specific standards for the design and placement of corona rings. Keeping that in mind, ring optimization for a 1000 kV composite insulator is performed. Also, the effect of grading rings on non-linear EFVD along composite insulators used in UHV systems is analyzed.

To study the effect of the tower configuration, electric field analysis on composite insulators is carried out in dead end and suspension environments for voltage rating ranging from 138 kV to 500 kV ac. Dead end structures can consist of a single or double circuit. The effect of the number of circuits on the electric field distribution along composite insulators is also investigated.

The electric field analysis can be done with the help of laboratory tests, analytical techniques or numerical techniques. Laboratory tests are extremely time consuming and can be very expensive. These might require several rounds of testing in order to obtain accurate results. Analytical techniques can be carried out for simple models but when the model complexity increases these prove to be very rigorous and time consuming. With the computing power available today, it is relatively simple to carry out extensive modeling of the most complex geometries. Several commercially available software packages based on the concepts of Finite Element Analysis

(FEM), Charge Simulation Methods (CSM) and Boundary Element Methods (BEM) are available. For the purpose of this research, COULOMB 8.0 – field design and analysis software based on the concept of BEM is used. This has been provided by Integrated Engineering Software (IES). Also, EPRI developed software EPIC based on the concept of CSM is used.

1.2 Research Objectives

The work done here focuses on the determination of the performance of composite insulators with the help of software tools. This contributes towards the design process of Extra High Voltage and Ultra High Voltage insulators where performing laboratory tests could prove to be extremely expensive and time consuming. The major research objectives are stated below:

1. Performing calculations to determine the electric field distribution along different composite insulators rated from 138 kV up to 1200 kV ac, under wet and dry conditions. These calculations help in ascertaining the possibility of flashover in designing appropriate flashover or corona mitigation techniques.
2. Analysis of the effect of corona rings and bundled conductors on the electric field distribution along composite insulators of different ratings. These help in choosing appropriate ring dimensions and also the optimum number of conductors that should be used per bundle in order to keep the electric field under acceptable limits.
3. Another objective is to optimize the corona ring parameters namely, the ring diameter, ring tube thickness and the projection of the ring form the high voltage energized end fitting for use in UHV systems. Corona ring with optimized parameters is designed and modeled on a 1000 kV UHV system.
4. Analyzing the effect of grading rings on electric field and voltage distribution along composite insulators used for UHV (1000 kV and 1200 kV) systems. Demonstrating the improvement in the EFVD with the help of these large grading rings around two parallel units of composite insulators (double insulator string).

5. Determining the difference in the electric field calculations for suspension and dead end composite insulators for system voltages ranging from 138 kV to 500 kV ac. This difference was also studied as a function of the system voltage.
6. Analysis of electric field distribution along composite insulators used in single and double dead end configurations for a 230 kV ac rated system voltage.

1.3 Organization of this Thesis

The work presented here is divided into seven chapters. In chapter 1 and 2, the overview of this research work and a literature summary of related topics: basics of insulators, types of insulators and failure modes are discussed. Chapter 3 describes various methods of electric field calculations with special emphasis on the ones that are used for the work presented here. Chapter 4 describes in detail the composite insulators modeled along with the techniques employed for modeling. Results of electric field calculations made under dry and wet conditions as well as the effect of corona rings and bundled conductors on the electric field distribution along composite insulators is discussed. Chapter 5 presents electric field analysis performed on EHV and UHV composite insulators including optimization of corona ring and the effect of grading ring on the linearity of EFVD along composite insulators. In chapter 6, work carried out using the software EPIC which includes modeling composite insulators in suspension and dead end environments for system voltages ranging from 138 kV to 500 kV ac are discussed. The modeling techniques used in software EPIC are briefly discussed. Also, modeling carried out on single dead end and double dead end composite insulators for a 230 kV system is presented.

2. LITERATURE REVIEW

2.1 Introduction

Outdoor insulators form an integral part of power transmission systems. These perform the dual function of mechanical support to the line conductors as well as electrically isolating them from the tower structure [1]. This section is aimed at providing an insight into the available literature on different types of insulators already in use and also account for different reasons for failure of insulators. The first part of the chapter is dedicated to an overview of the different insulating materials used for manufacturing insulators and the different configurations available. Following this is a description of the different modes of failures on insulators. These are discussed in detail.

2.2 Types of Insulators

By definition, an insulator is an insulating material designed to support a conductor physically as well as electrically separate it from other conductors or objects [20]. The basic parts of an insulator are:

- Dielectric
- Metal end fittings
- Internal parts

There is a variety in the type of construction methods used as well as the kind of materials employed for construction. The use of different kinds of insulators is based on the application and the environment conditions. There are different dimensions and designs based on the voltage rating for which they are used. Broadly, insulators can be divided into different classes based on the kind of dielectric material used for their construction which are as follows:

2.2.1 Porcelain Insulators

Porcelain insulators fall in the category of ceramic insulators. These have been used in the power industry for more than a century and are still the most widely used. Porcelain insulators are relatively heavy and brittle. These consist of a string of porcelain sheds with each shed made up of a metal cap, a metal pin and porcelain shed. The number of sheds used varies with the system voltage and these are well documented in the EPRI transmission line reference book. Porce-

lain material is hydrophilic in nature, i.e. water forms a thin film on the surface of the insulator. The different insulator configurations are:

- Cap and pin insulator
- Station post insulators
- Transformer and circuit breaker bushings

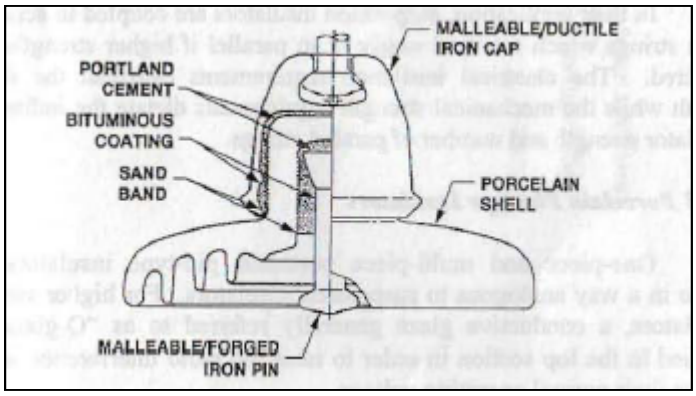

Figure 1. Cap and pin insulator (directly taken from [1])

Porcelain insulators are generally glazed for making the surface of the insulator smooth. This helps in reducing localized corona discharges at sharp edges. The glaze is chemically inert and therefore resists surface corrosion.

2.2.2 Glass Insulators

Insulators made from glass were in use for telegraph lines even before they were employed for power transmission lines [1]. The different kinds of insulator configurations made form glass are:

- Glass suspension insulator
- Glass pin type insulator
- Glass multicone post insulator

The main difficulty in using glass is that flaws in the surface often lead to fracture under stress. Processes like thermal tempering or toughening are carried out to improve the strength characteristics of glass material [1]. These are often prone to vandalism.

2.2.3 Non-ceramic Insulators

The demand of electrical energy has been ever increasing with time. In order to cater to the needs of customers, it was required to upgrade or install new transmission lines at even higher voltages. The dimensions of the insulators used for these lines increased and consequently the weight also increased. The quest for designing insulators with reduced weight and improved mechanical and electrical characteristics lead to the development of non ceramic insulators. The last few years have witnessed the replacement of porcelain with polymer materials such as silicone rubber. This is attributed to multiple advantages that they have over porcelain. Polymer materials have excellent pollution performance and hence are suitable for high polluted areas.

Non ceramic insulators are usually made up of silicone rubber, Poly-Tetra -Fluoro-Ethane (PTFE) or Ethyl Propylene Diene Monomer (EPDM) rubber. Non ceramic insulators consist of the following main parts:

- Fiberglass rod: Provides the main mechanical frame and at the same time is also the main insulating material in the geometry. This rod consists of axially aligned, 70-75 % by weight of 'E' type glass fibers [1].
- Silicone rubber housing: The fiberglass rod is enclosed in silicone rubber housing with weather sheds. The polymer material is shaped and spaced over the rod in various ways to protect it from the environmental conditions.
- Metallic end fitting hardware: The end fitting hardware is generally made form cast or forged aluminum, iron or steel [1]. Various techniques have been developed to attach this end fitting to the core for optimum electrical performance.

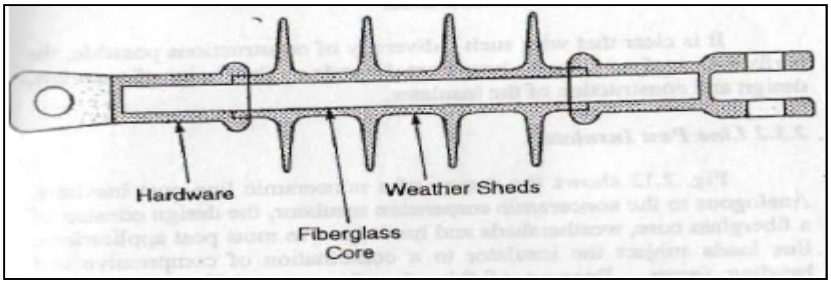

Figure 2. Non-ceramic suspension insulator (directly taken from [1])

Composite insulators/bushings, especially made from silicone rubber samples with hydrophobic surfaces, have discrete water droplets rather than thin film of water on their surfaces under moist conditions (rain, fog etc). Therefore, the insulator provides a high resistance path to the flow of leakage current. This helps in reducing the probability of flashover [21].

2.3 Causes of Failure

This section presents an overview of the different causes that lead to the failure of composite insulators in particular:

2.3.1 Handling

Mishandling of composite insulators during transportation can lead to their failure. Contact with sharp objects or abrasive surfaces can cause damage to the housing material. During installation, the composite insulator might be subjected to tension due to torsion or cantilever load which could lead to cracking of the core [1]. Any kind of physical damage to the outer housing material makes the fiberglass rod vulnerable by exposing it to the environmental conditions like moisture, pollution etc. This could lead to tracking along the core and brittle fracture.

Equipments that are extremely damaged are not installed but there might be cases of cracks and fractures that are invisible to the naked eyes. Installation of such specimen might lead to failure during operation. Hence, utmost care should be taken in packing these samples during transportation as well as installation.

2.3.2 Vandalism

Composite insulators are less prone to damage related to vandalism unlike porcelain and glass. These are capable of withstanding severe gunshot damage without any immediate electrical or mechanical failure. However, if the gunshot exposes the fiberglass rod to the environment, failure might occur due to tracking along the rod or brittle fracture. Regular inspections should be carried out in regions that are prone to vandalism in order to prevent any misoperation due to insulators affected by gun shots.

2.3.3 Manufacturing Defects

Many failures do arise from inadequate quality standards during manufacturing stage of composite insulators. Generally, end fittings are attached to the core by the process of swaging [1]. Care should be taken to carry out this process such that no damage is caused to the core. The tolerances between the outside core diameter and the inside hardware diameter should be optimum in order to reduce the risk of crack in the hardware due to swaging. Bonding of the polymer housing to the core post injection molding may be insufficient due to incorrect core preheat temperature, moisture in the form of humidity, incorrect mold temperature etc [1]. Care should be taken to maintain these variables within acceptable limits.

2.3.4 Flashover

As per the standard definition, flashover is defined as a disruptive discharge though air or over the surface of solid insulation, between parts of different pollution or polarity produced by the application of voltage wherein the breakdown path becomes sufficiently ionized to maintain an electric arc [20]. A few factors that could cause flashover are switching surge, lightning impulse and contamination:

- *Flashover caused due to Switching surges and lightning impulses:*

When impulse surges are applied to air gaps, the breakdown process consists of three major stages: corona development, formation of leader channels and finally the main stroke. The formation of corona happens almost instantaneously in a fraction of a microsecond. This might be followed by a second burst of corona depending on the magnitude and rate of rise of the applied voltage. If the voltage is high enough to develop a leader channel which crosses the gap, breakdown will occur. The formation of the leader channel is the main criterion for flashover of the gap [25].

- *Flashover caused due contamination:*

Polymer material is hydrophobic in nature and hence resists the formation of a film of water on its surface. Instead water beads up in the form of small droplets and does not wet the entire surface. This reduces the leakage current and probability of forming dry bands which im-

plies better performance. However, the hydrophobicity of these materials might be destroyed temporarily due to heavy pollution in addition to wet conditions thus increasing the leakage current. However the surface recovers hydrophobicity post 10-12 hours of dry and arc free period [22].

Figure 3. Composite insulator showing water droplets

The mechanism of flashover phenomenon for composite insulators is different from the ones suggested for porcelain and glass insulators, as suggested by Karady et all. The mechanism is briefly discussed here. Surface contaminant particles like salt spray, emissions from industries and automobile exhaust fumes are generally driven towards the surface of the insulator though wind. Fog, mist or light rain wets these deposits thereby making the contamination layer conductive resulting in a leakage current. The composite insulator is now covered by a high resistive layer, which is scattered with conducting droplets. The water droplets are often elongated in the presence of high electric field [23]. The neighboring droplets may coalesce and form small filaments which are conductive in nature. These conductive spots are surrounded by regions of high resistance. There might be localized spot discharges around these filaments due to electric field intensification which affect the hydrophobicity of the material. Gradual increase in filament length and formation of wet areas increase the conductive path on the surface on the insulator and might short it. The conductive path enhances the chances of formation of an arc which might travel on conductive surface of the insulator causing flashover [24].

2.3.5 Corona Degradation

Another phenomenon that affects the electrical and mechanical performance of composite insulators is corona. Corona is caused due to high electric fields on the surface of the insulating material. High electric fields have the tendency to accelerate the free electrons around the insulator. The collision of atoms of air and the fast moving electrons cause a phenomenon known as electron avalanche. The number of free fast moving electrons increases exponentially which leads to the air around the insulator to get ionized. This causes corona discharge. Under dry conditions, if the electric field exceeds the threshold of 1.5 kV/mm, chances of corona discharge are very high [4]. However, in wet conditions corona is seen at lower electric field magnitudes. The threshold electric field magnitude for the corona discharge not only depends on the condition of the surface (dry or wet) but also on the type of applied voltage (ac or dc). Manufacturing defects or rough and sharp edges are regions of high electric stress. This localized high electric stress could also cause corona discharge.

The mechanical impact of ions is capable of causing mechanical damage to the insulator. The generation of hydrated nitrogen oxides, through secondary reactions, form acidic water on the insulator surface on dissolving with water. The presence of acidic water might lead to corrosion of the insulator surface. The presence of corona is an indication of high electric field making the insulator vulnerable to damage caused by flashover. In worst case, continuous corona could lead to line loss.

The electric field at the triple junction formed by the dielectric material, the end fitting and air is usually very high. This is further enhanced by the presence of water droplets along the length of the composite insulator. A water droplet plays a number of roles in the electrical breakdown of air and insulating material junction [26]. Firstly, it enhances stress due to its high permittivity. Secondly, it undergoes deformation in the presence of an electric field. The elongation of water droplet by electrostatic forces results in immediate increase in electric field at the drop tip, causing corona. Thirdly, it is a good conductor in the presence of contamination and hence shorts out some of the insulating surface of equipment. The corona inception voltage depends on the

volume of the water droplets, the conductivity of the water, the contact angle that the droplet makes with the surface of the insulator, which is a property of the hydrophobicity of the material [27].

2.3.6 Voltage Stress

The potential distribution along composite insulators is highly non-uniform as a result of absence of any distributed or stray capacitance, unlike porcelain insulators [1]. The voltage stress is a function of line voltage and does not depend on the length of the insulator. Corona discharge is a consequence of voltage stress which can hamper the electrical and mechanical performance of the composite insulator. Therefore the knowledge of the voltage and electrical stress along composite insulators or any high voltage equipment for that matter is very essential in order to improve the performance of the equipment.

This research is dedicated to analyzing electric field and potential distribution along composite insulators used in transmission systems under different conditions. Also, ways to mitigate the high electric fields are presented. The problem of non linearity of the electric field and voltage distribution, especially along composite insulators used for UHV transmission system, is studied and a solution to improve the EFVD along the length of the composite insulator is suggested.

3. ELECTRIC FIELD ANALYSIS TECHNIQUES

3.1 Introduction

Knowledge of electric field and potential distribution along high voltage insulators is of great importance in the design, operation and performance of the equipment. There are various methods of electric field calculations. Several techniques can be used for the analysis of electric fields. They can be categorized into experimental field analysis methods, analytical methods and numerical analysis methods. These methods have their own advantages and disadvantages; therefore it is advisable to choose a suitable method as per the requirements of the analysis. For a long time, laboratory experiments were performed to calculate the electric field along insulators due to the lack of efficient computational techniques. Analytical methods are suitable for simple geometries. With the computing power available today, numerical methods can provide accurate electric field calculations along high voltage equipment. Numerical methods are highly recommended for initial design stages of composite insulators used in EHV and UHV systems in order to avoid the high cost of running laboratory tests. Therefore, in design and analysis of high voltage equipment, selection of an efficient technique for electric field analysis is very essential. This section aims at providing an overview of the different electric field analysis techniques that exist. For the purpose of this research, boundary element method has been used.

3.2 Experimental Field Analysis Technique

Experimental field analysis techniques are methods in which the real physical system is replaced by an analogue one, where the quantities are much easier to measure [28]. Laboratory tests are performed to measure the electrical field across the insulators. These are done under different simulated environments. Laboratory tests take care of the factors that cannot be modeled easily. With the computing power available today, electric field analysis along insulators can be calculated very easily. However, laboratory tests are still carried out in order to validate the results obtained from computer simulations. The different methods used to calculate the electric field experimentally are briefly described below:

3.2.1 Impedance Networks

Impedance networks can be defined as dividing the contiguous resistive medium into small blocks and replacing them by lumped resistance of adequate magnitude [28]. The concept of impedance networks leads to a finite difference approximation to the differential operators and therefore inherits errors because of the imperfections of the finite difference methods. The resistance network analogue used in this system can approximate Laplace's equations and Poissonian fields. The application of this method for solving electrostatic fields in high voltage equipments is not very useful.

3.2.2 Electrolytic Tank

Electrolytic tank analysis technique consists of a simple tank constructed from insulating material filled with a conducting fluid. The electrodes for which the potential distribution is to be determined are immersed in the fluid. The electric potential is determined using probes. Three dimensional problems are difficult to simulate using this method.

3.3 Analytical Field Analysis Techniques

Analytical techniques are recommended for relatively simpler geometries where the conducting surfaces are cylinders, spheres etc [29]. These make use of developed formulae to calculate the electric field along a simple geometry. For complex geometries, which is generally the case with high voltage equipment, the analytical expressions get extremely complicated and the analysis becomes cumbersome. Numerical methods of field analysis, using computer software, are replacing all other methods of electric field analysis.

3.4 Numerical Field Analysis Techniques

Numerical methods are used to determine the electric field distribution for complex geometries, where it is cumbersome and expensive to use analytical techniques or run laboratory tests. All electromagnetic field problems can be expressed in terms of partial differential equations with the help of Maxwell's equations [29]. Along with these set of equations, certain boundary

conditions are described in order to completely describe the electric field for the system under consideration. The Maxwell's equations are as follows:

In free space, Maxwell's equations and the constitutive equations are [29]:

$$\nabla \times H = \frac{\partial D}{\partial t} + J$$

$$\nabla \times E = -\frac{\partial B}{\partial t}$$

$$\nabla . B = 0 \qquad (1)$$

$$\Delta . D = \rho$$

$$B = \mu H$$

$$D = \mu E$$

In the presence of conducting materials, the principle of charge conservation is expressed by the relation [29]:

$$\nabla . J + \frac{\partial \rho}{\partial t} = 0 \qquad (2)$$

The variables used are described below:

- H = Vector of magnetic field strength
- E = Vector of electric field strength
- B = Vector of magnetic flux density
- D = Vector of electric flux density
- J = Conduction current density
- ρ = Electric charge density
- □ = Permittivity of free space
- μ = Permeability of free space.

At the interface of different materials the integral from of Maxwell's equations is reduced to [29]:

$$\begin{aligned} n.(B1 - B2) &= 0 \\ n.(D1 - D2) &= \sigma \\ n \times (E1 - E2) &= 0 \\ n \times (H1 - H2) &= K \\ n \times (J1 - J2) &= -\frac{\partial \sigma}{\partial t} \end{aligned} \tag{3}$$

Where:

- n = Unit normal vector to the interface of surfaces 1 and 2
- B1, D1, E1, H1, J1 = Field vectors on surface 1
- B2, D2, E2, H2, J2 = Field vectors on surface 2
- K = Density of surface currents
- σ = Density of surface charges

By using Green's function, these partial differential equations can be transformed into differential or integral equations. The purpose of numerical methods is to transfer an operator equation, differential or integral, into a matrix equation. These are solved iteratively till the solution converges with a certain predefined tolerance limit. There are two different categories of numerical methods: The domain methods and the boundary methods [29]. Domain methods make use of differential equations whereas boundary methods make use of integral equations in their solver. The different domain methods are Finite Element Method (FEM) and Finite Difference Method (FDM); while the boundary methods include Charge Simulation Method (CSM) and Boundary Element Method (BEM).The work presented here makes use of computer software based on Boundary Element Method (BEM). This method employs integral equations and the principle of weighted residuals for calculations. Volume integral is transformed into surface inte-

gral, thereby reducing the dimension of the problem by an order of one. The various numerical techniques mentioned above are discussed briefly in the sections that follow.

3.4.1 Finite Difference Method

This method is an approximation for solving partial differential equations. This can be applied to linear, non –linear, time independent and dependent equations. In this method, the solution domain is divided into many nodes in a regular grid. The partial derivatives of unknown functions are approximated by the difference quotients. Methods like Taylor's series are used to transform the differential operator into difference operator. According to Laplace's equations, potential at any node in a mesh is given by:

$$\frac{\partial^2 V}{\partial r^2} + \frac{1}{r}\frac{\partial V}{\partial r} + \frac{\partial^2 V}{\partial z^2} = 0 \tag{4}$$

The finite difference form of this equation is given by:

$$V_{r,z} = K_1 V_{r+1,z} + K_2 V_{r-1,z} + K_3 V_{r,z+1} + K_4 V_{r,z-1} \tag{5}$$

Where the co – efficients k_1, k_2, k_3, k_4 depend on the model geometry and mesh configurations. The application of this method is relatively easy. However, the elements need to be rectilinear which implies that convoluted geometries are not discretized accurately enough.

3.4.2 Finite Element Method

Finite element analysis is an example of domain method. The method is based on the concept of obtaining differential equations after applying Green's theorem to Maxwell's equations [29]. The idea is to divide the solution domain into a number of small interconnected elements. The following steps describe the FEM:

- Discretization of the solution domain into smaller regions. Considering triangular elements, the unknown function μ is approximated by the nodal values μ_i, μ_j, μ_m and the shape function $N^e{}_k$:

$$\mu_e = \sum N_k^e \mu_k \tag{6}$$

- With the help of the principle of weighted residuals, the element matrix equation is derived. The matrix equation for triangular elements is represented as:

$$\begin{bmatrix} K_{ii} & K_{ij} & K_{ik} \\ K_{ji} & K_{jj} & K_{jk} \\ K_{ki} & K_{kj} & K_{kk} \end{bmatrix} = \begin{bmatrix} \mu_i \\ \mu_j \\ \mu_k \end{bmatrix} \quad (7)$$

Where k is the co-efficient of μ obtained by weighted least squares methods.

- The system matrix equation is obtained by assembling the element matrix equations.

$$K\mu = B \quad (8)$$

Where μ is the column matrix with order N, where N is the number of nodes, containing all the nodal values of the domain. Matrix K is of order N x N and is sparse, symmetric and positive definite in nature. The column B contains the source terms included in Poisson's equations and the known boundary conditions.

FEM is very flexible and can be applied to the most complicated geometries. It is capable of giving highly accurate results and the accuracy of results depends on the number of elements considered in the geometry. The main disadvantage of this method is that the entire domain space is divided into elements. In case of unbounded regions, the number of elements considered becomes extremely large which in turn increases computation burden. There could also be large localized errors with no means to check the accuracy of the results.

3.4.3 Charge Simulation Method

Charge simulation method has been used for many high voltage problems. It falls under the category of boundary methods. This method works by replacing the distributed charge of conductors as well as the polarization charges on the dielectric interfaces by a large number of fictitious discrete charges [29]. The magnitudes of these charges are calculated such that their integrated effect satisfies the boundary conditions exactly at a selected number of points on the boundary. An advantage is that it can be applied to three dimensional field problems without axial symmetry.

The first step in solving a problem by charge simulation method is to find out the equivalent simulated charges by the charge simulation equation. These charges are always located outside the domain of field distribution calculation. After determination of these lumped charges, the solution of potential and electric field strengths anywhere in the domain are computed by the analytical formulation and the superposition principle. However, care should be taken to avoid singularity when the point at which the potential is being calculated is the same as the point at which the calculated charge is present.

For instance, let Q_k be a lump of a number individual charges n, and φ_i be the associated potential at any point P within the space. According to the superposition theorem:

$$\varphi_i = \sum_{k=1}^{n} P_{ik}\, Q_k \tag{9}$$

Where P_{ik} are the potential coefficients which can be found out by solving Laplace's or Poisson's equations. Let Q_1, Q_2, Q_3 be three point charges in space. Let the potential at a point X_1 be measure and given by φ_k. Therefore:

$$\varphi_k = \frac{Q_1}{4\pi\varepsilon R_1} + \frac{Q_2}{4\pi\varepsilon R_2} + \frac{Q_3}{4\pi\varepsilon R_3} \tag{10}$$

$$\varphi_k = P_{K1}Q_1 + P_{K2}Q_2 + P_{K3}Q_3 \tag{11}$$

A relationship between potential and charge at each point is established. The matrix equation solved to get the solution for the charge simulation method is [29]:

$$\begin{bmatrix} P_{11} & . & . & P_{1n} \\ . & . & . & . \\ . & . & . & . \\ P_{m1} & . & . & P_{mn} \end{bmatrix} \begin{bmatrix} Q_1 \\ . \\ . \\ Q_n \end{bmatrix} = \begin{bmatrix} \varphi_1 \\ . \\ . \\ \varphi_2 \end{bmatrix} \tag{12}$$

With the assumption that there are N conductors with known potential in a single dielectric medium, the actual charges on the surface of these conductors are replaced by n_a fictitious charges placed inside or outside the conductors. In order to calculate the magnitude of these charges, n_b points are selected on the surface of these conductors. The condition that should be satisfied is that the known conductor potential should be equal to the potential resulting from su-

perposition of all the simulation charges, at any of the contour points. The charges are determined from [29]:

$$[P]_{nxn}[Q]_{nxn} = [\varphi]_n \quad (13)$$

Where, [P] is the potential co-efficient matrix

[Q] = Column vector of values of unknown charges

[φ] = Potential of boundary points

After equation (14) is solved for magnitude of simulation charges, it is essential to verify whether the set of calculated charges produce actual boundary conditions on the electrode surface. The charge simulation method does not require the entire domain to be divided into elements. This reduces the computation burden. The required electric field or potential at any particular point can be calculated easily using the principle of superposition once the simulated charges are calculated. Extreme care should be taken to avoid a source at the position where the potential is to be calculated in order to avoid any errors due to singularity.

3.4.4 Boundary Element Analysis

The work presented here makes use of the software package COULOMB based on the concept of boundary element method. This is based on boundary integral equations and the principle of weighted residuals. Calculations for the potential function are made by calculating an equivalent source which sustains the required electric field at a given point. It is mandatory for the function to satisfy the boundary conditions. The most important feature of boundary element method is that it requires discretization of surfaces rather than volume. This decreases the order of the problem and also gives more accurate results.

The expansion and testing functions as well as the geometry is are specified on an element by element basis. Expansion function co-efficients are defined at nodes on the element. The software package COULOMB uses linear shape functions defined over each element [9]. These are expresses as follows:

$$\beta_1 = \mu - \tau\mu \quad (14)$$

$$\beta_2 = 1 - \tau - \mu + \tau\mu \tag{15}$$

$$\beta_3 = \tau - \tau\mu \tag{16}$$

$$\beta_4 = \tau\mu \tag{17}$$

The charge at each element is given by:

$$\sigma = \sum_{i=1}^{m} \sigma_i \beta_i(\tau, \mu) \tag{18}$$

COULOMB models the geometry by fitting Lagrangian shape function to the specified surface given as:

$$\beta_1 = \tau\mu(2\tau - 2) + \mu(1 - \tau)(2\mu - 1) \tag{19}$$

$$\beta_2 = \tau(1 - \mu)(2\tau - 1) + (1 - \tau)(1 + \mu(2\mu - 3)) \tag{20}$$

$$\beta_3 = \tau(1 - \mu)(2\tau - 2) + \tau(1 + \mu(2\mu - 3)) \tag{21}$$

$$\beta_4 = \tau\mu(2\tau - 2) + \tau\mu(2\mu - 1) \tag{22}$$

$$\beta_5 = 4\mu(1 - \tau)(1 - \mu) \tag{23}$$

$$\beta_6 = 4\tau(1 - \tau)(1 - \mu) \tag{24}$$

$$\beta_7 = 4\tau\mu(1 - \tau) \tag{25}$$

$$\beta_8 = 4\tau\mu(1 - \tau) \tag{26}$$

Global positions in cartesian system are specified over each element as:

$$x = \sum_{i=1}^{m} \beta_i(\tau, \mu) x_i \tag{27}$$

$$y = \sum_{i=1}^{m} \beta_i(\tau, \mu) x_i \tag{28}$$

$$z = \sum_{i=1}^{m} \beta_i(\tau, \mu) z_i \tag{29}$$

From the method of weighted residuals, $\langle w_m, K\Phi_n \rangle = \langle w_m, b \rangle$ has to be determined. The operator K is dependent upon the boundary conditions where the inner product needs to be calculated. In the case of Dirichlet sections of the boundary,

$$K\sigma = \Phi(r) = \int G(\bar{r}, \bar{r}')\sigma(\bar{r}')ds' \qquad r \in Bi\,\mathrm{r} \tag{30}$$

Substitution of the shape functions for the equivalent sources results in:

$$K\beta^T\sigma = \int G(\bar{r}, \bar{r}')\beta^T(\bar{r}')ds'\sigma = \Phi(\bar{r}) \tag{31}$$

In the case of Neumann sections of the boundary, inner product produces:

$$\beta(r) = \int G(\bar{r}, \bar{r}')\beta^T(\bar{r}')ds'dr\sigma + 2\pi \int \beta(\bar{r})\beta^T(\bar{r})dr\sigma \tag{32}$$

The software package COULOMB applies the appropriate inner product for each element, depending on the boundary conditions. A major difficulty in the integral equation approach is the integration of green function singularity. This occurs when the observation points coincide with the source points being calculated. COULOMB handles this singularity by further dividing the singularity and using different transformations in order to remove them [9]. These may require mathematical or coordinate transformations.

For the analysis of electric field in insulators, Boundary Element Analysis is an efficient method. It gives high accuracy while decreasing the dimensionality of the problem by one. Generally, insulators are rotational symmetric. COULOMB makes use of this advantage by considering only angular sections of the entire geometry for calculations. This reduces the computation time significantly. Also, there are means to check the accuracy of results. Integration performed on the electric field graph obtained gives the applied potential across the equipment. The difference in the value obtained and the applied voltage gives the error factor. For the purpose of this work, the error factor was maintained below 5%.

However, a there are a few disadvantages of Boundary Element Method. Sometimes, integrals can produce a singular matrix. Care must be taken to avoid such a situation or to handle it appropriately. The method is not applicable to non-linear problems directly.

4. ELECTRIC FIELD ANALYSIS OF COMPOSITE INSULATORS

4.1 Introduction

In order to meet the ever increasing demand for electric power, many utilities are either building new transmission systems or upgrading the existing ones to higher capacity. Insulators made from porcelain have been in use for a long time. The last few years have witnessed the replacement of porcelain with polymer materials such as silicone rubber. This is attributed to multiple advantages that they have over porcelain. Polymer materials have excellent pollution performance and hence are suitable for highly polluted areas. Lead time is reduced owing to the fact that composite insulator manufacturers have increased significantly in the last few years. They are also light weight, easy and economical to transport and install. Also, these are not brittle in nature as against porcelain type. However, there are manufacturing constraints as the size of these insulators increases with the voltage rating. This puts greater mechanical and electrical stress on high voltage insulators. This section is dedicated to analyzing how the electric field distribution along composite insulators changes with increase in voltage rating, under different conditions like dry and wet. The effect of corona rings in mitigating high electric fields is also studied. The analysis also includes the effect of bundled conductors on the electric field distribution along composite insulators.

4.2 Composite Insulators Dimensions

Composite insulators are considered for the purpose of this research. Insulators of different dimensions are used for different voltage ratings, keeping in mind the mechanical stress that they need to handle. Dimensions for 138 kV and 230 kV systems were taken from EPRI's Task Force on modeling composite insulators and Salt River Project respectively. Insulator dimensions for voltage rating from 345 kV to 1000 kV were taken from the catalog provided by Xinjiang New Energy [5]. Catalog information for 1200 kV composite insulator was not available and this was obtained by extrapolation.

Table 4-1. BIL and SML levels of insulators used at different voltage rating

Voltage rating (kV)	BIL (kV)	SML (kN)
138	#	#
230	#	#
345	1425	100-210
500	2250	100-400
765	2700	100-400
1000	3200	210-420
1200	*	*

*Catalog information not available

Table 4.1 shows the Basic Lightning Impulse Insulation Level (BIL) and the Specified Mechanical Load (SML) of insulators used for different voltage ratings. BIL is defined as the crest value of a standard lightning impulse for which the insulation exhibits a 90% probability of withstand under specified conditions applicable for self-restoring insulation [1]. Insulators are defined in terms of Mechanical and Electrical (M&E) strength, also known as SML, which is determined by subjecting the insulator to a tensile strength test while it is energized at 75% of rated dry low frequency flashover voltage specified for the particular model [8]. The range of tensile load for an individual specimen is specified in the manufacturer's catalog. The weight of the sample varies according to the tensile load that it can bear.

Table 4-2. Dimensions for composite insulators at different voltage ratings (taken from [5], [6], [7])

Voltage rating (kV)	Dry arc distance (mm)	Leakage distance (mm)
138	1042	2809
230	2000	5815
345	2600	9075
500	5000	13750
765	6600	23500
1000	7110	25550
1200	8530	30660

Table 4.2 shows the dry arc distances and leakage distances used for electric field calculations along insulators at different voltage ratings. Dry arc distance is defined as the shortest distance through the surrounding medium between terminal electrodes, or the sum of the distances

between intermediate electrodes, whichever is shorter. Leakage or creepage distance is defined as the sum of the shortest distances measured along the insulating surfaces between conducting parts as shown in Figure 4 [1].

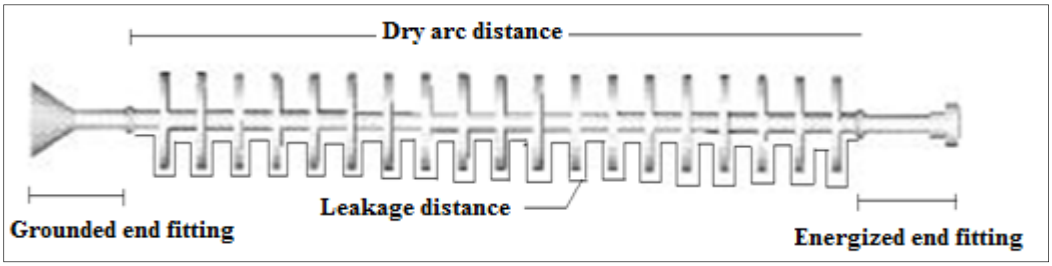

Figure 4. Dry arc distance and leakage distance along a composite insulator

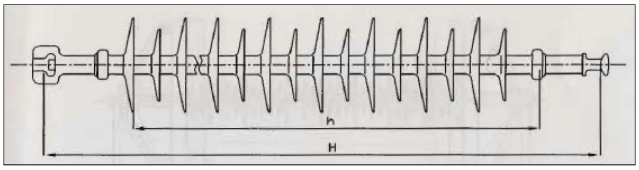

(a)

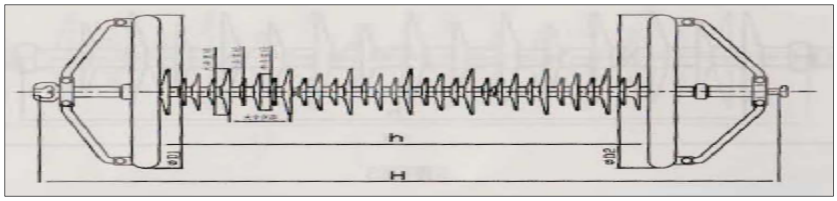

(b)

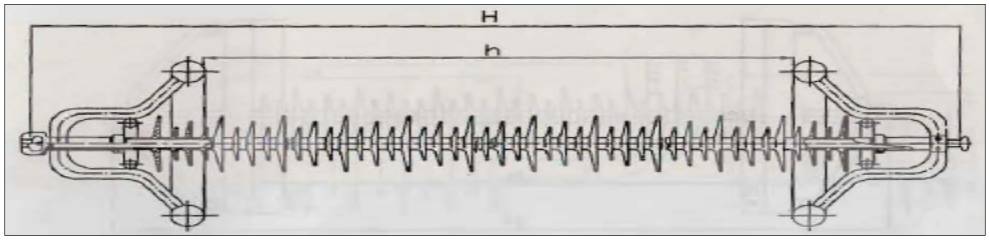

Figure 5. Schematic used in COULOMB 8.0 for composite insulator of following voltage ratings (a) 138 kV (b) 500 kV and (c) 1000 kV [Directly taken from manufacturer catalog]

In the figure above, H denotes the total connection length whereas h denotes the dry arc distance.

4.3 Base Case – Electric Field Analysis under Dry Conditions

The three – dimensional software COULOMB 8.0 was used to calculate the electric field distribution along composite insulators. The numerical analysis was carried out on a workstation with 3.16 GHz processor, 4GB RAM. The process of calculation involves some specific steps which are discussed in the sections that follow:

4.3.1 Modeling Insulator Geometry

Taking advantage of the fact that the composite insulators are rotational symmetric, only angular sections are modeled. For all dry cases, the entire 360 degree section is considered. The simulation files are as large as 4 to 5 MB in size. For wet cases, the presence of water droplets all along the length of the hydrophobic material of the composite insulator make the file size very large, in the order of 20 to 30 MB. In order to reduce computation time without affecting the accuracy, only angular sections are considered. For voltage rating from 138 kV up to 500 kV, 30° angular section is considered. While only 20° section of the insulator rated at 1000 kV is considered.

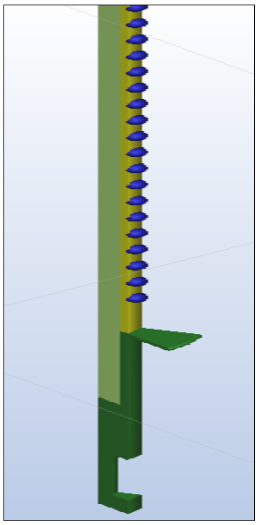

Figure 6. Schematic of an angular section of a 138 kV composite insulator modeled in COULOMB

4.3.2 Assigning Material Properties

The different parts of the model are assigned different materials. Table 4.3 lists basic properties like relative permittivity and thermal conductivity of the materials used:

Table 4-3. Properties of different materials used for modeling

Material	Relative permittivity	Thermal conductivity (Mho/m)
Silicone	3	1e-017
Fiberglass	5	1e-012
Steel	1	1670000
Water	80	0.0002

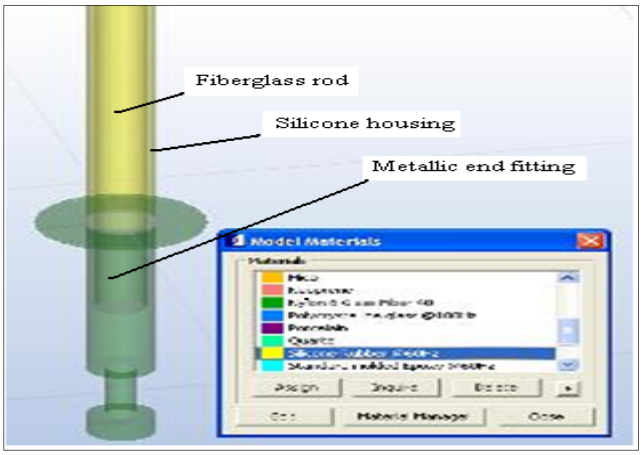

Figure 7. Assigning material properties to different parts of composite insulator in COULOMB

4.3.3. Assigning Boundary Conditions

Boundary conditions include assigning the rated line-to-ground voltage to the energized high voltage end fitting and 0 volts to the grounded end fitting of the composite insulator. The next step is to define the angular periodic sections. For the ease in construction of the model and reduction in the computation time, only angular sections of the rotational symmetric model are considered. It is essential to specify the section angle and also the number of sections required to complete one insulator. The number of sections is given by 360° divided by the angle of the section considered.

4.3.4 Assigning Boundary Elements

The boundaries in the model need to be discretized into individual sections, referred to as boundary elements. The distribution, number and shape of these elements are the key factors that determine the accuracy of the solution. BEM generally uses 2D elements for analysis purpose. For the purpose of this research, 2D triangular elements were chosen as it is relatively simple to assign 2D triangular elements to any surface when compared to 2D quadrilateral elements which can be assigned to only four sided surfaces.

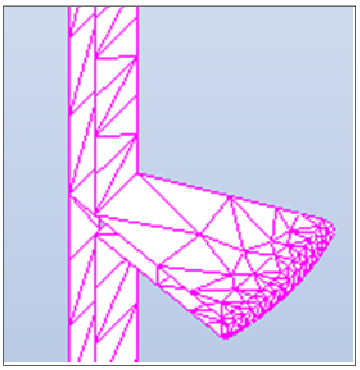

Figure 8. Triangular boundary elements assigned along a composite insulator under dry conditions

The accuracy of the results obtained gets better with increasing the number of the elements assigned. In hindsight, this might cause an unreasonable increase in the computation time. Therefore, a trade-off between accuracy and computation time has to be made. Initial runs were carried out in order to establish the optimum number of 2D triangular elements keeping both these factors in mind. For this purpose, 138 kV rated composite insulator under dry conditions was modeled with 5000 evenly distributed triangular elements. This run gave reasonably good results in about 20 minutes whereas doubling the number of elements increased the computation time two fold, while only marginally improving the accuracy. When the same was repeated for a larger model, a 1000 kV composite insulator, the computation time was increased fivefold whereas insignificant improvement in accuracy was observed. The number of elements considered for different insulator configurations are given in Table 4.4.

Table 4-4. Number of elements used for boundary element analysis of different composite insulators at different voltage ratings under dry and wet conditions

Voltage (kV)	Angular section modeled - dry case (degree)	Angular section modeled - wet case (degree)	Elements (dry case)	Elements (wet case)
138	360	30	3000	3305
230	360	30	3000	4205
345	360	30	3000	4705
500	360	30	3500	6225
765	360	20	3500	6630
1000	360	20	4000	7790
1200	360	*	4000	*

* Simulation was not possible due to large file size under wet conditions

When the number of elements increases beyond 8000, the computation time goes up to more than fifteen hours for large models, 765 kV and 1000 kV voltage rating, under wet conditions. Therefore, care has to be taken to limit the number of elements in order to reduce the computation burden and time.

4.3.5 Assumptions and Simplifications

A typical 500 kV composite insulator has more than 100 weather sheds and can be as long as four meter in length. In order to obtain accurate results, a large number of elements would be required in such a case. This number would further increase for wet conditions where water droplets in the order of hundreds are modeled along the length of the insulator. This would increase the computation time drastically. Therefore, some reasonable simplification of the model is required. The important parts of a composite insulator are fiberglass rod, polymer sheath on the rod, polymer weather sheds and the two end fittings. For all cases, the weather sheds were ignored. Justification for this came from the initial runs that were made on two different models of 138 kV rated composite insulator:

Model A) This model considered the fiberglass rod, polymer sheath on the rod, 19 polymer weather sheds and the two end fittings.

Model B) This model considered all the parts in model A except for the polymer weather sheds.

Comparison of the calculated results showed that the difference in the maximum value of the electric field for both the models was less than 2%. Model A required 5000 triangular elements whereas model B required only 3000 elements for similar accuracy. The computation time for the model with weather sheds was four fold when compared to that without weather sheds. Therefore, it was concluded that a good trade off could be made between model complexity and accuracy by considering model B. Therefore, the weather sheds were ignored for all cases.

While performing the simulations for the work presented here, the following factors were kept in mind [9]:

- All dielectric materials are assumed to be linear, i.e. the permittivity is constant and independent of the electric field intensity
- Assignment of volume charges is not incorporated for any case.
- Only surfaces and not segments are assigned boundary conditions.

4.3.6 Results for Dry Case

This section presents the electric field calculations for all voltage ratings, under dry conditions, without considering the effect of any corona mitigating technique. The electric field is calculated along a straight line starting 1 mm form the energized end fitting and culminating at the grounded end fitting. It is ensured that the measurement line is straight and also 1 mm above the surface of the composite insulator as recommended by EPRI.

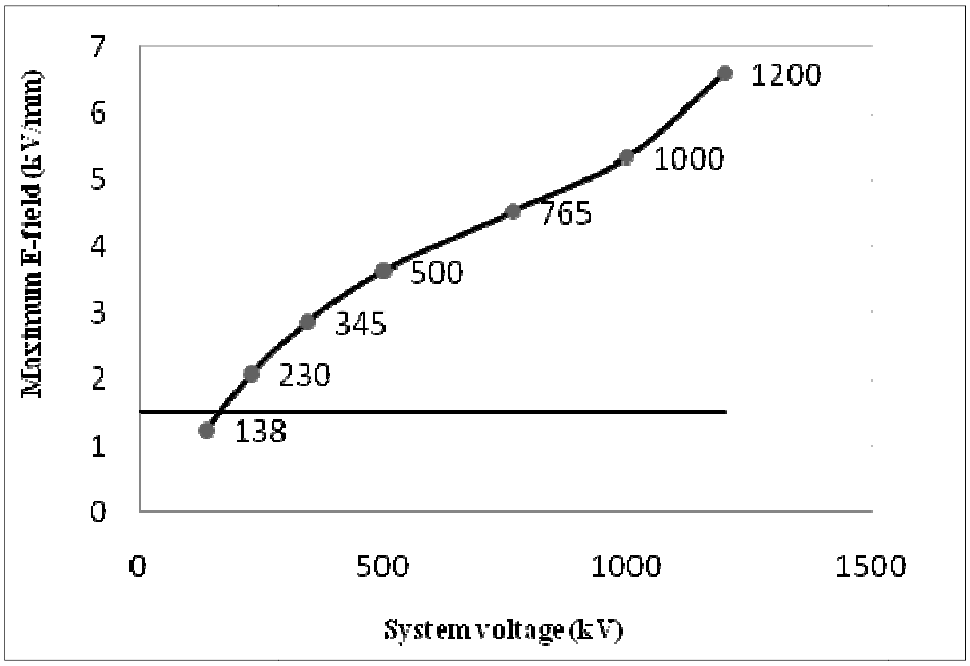

Figure 9. Maximum electric field along composite insulators under dry conditions as a function of system voltage

Figure 9 represents the maximum electric field value along the surface of the composite insulators under dry conditions as a function of system voltage. The maximum electric field value occurs at the triple point of the metallic energized end fitting- insulating housing material – air. Although the dry arc distance, along which electric field calculations are made, increases with the system voltage, the electric field stress along composite insulators at higher voltages is still higher. A value of 1.5 kV/mm is considered as the threshold for corona initiation [4]. From the results obtained, it is concluded that a corona mitigation device is required for system voltages 230 kV and above. The maximum electric field values for cases lesser than 500 kV were found to be relatively higher for composite insulators when compared to porcelain [10]. Also, composite insulators are more prone to corona related damage when compared to porcelain. Therefore, mitigation devices like corona rings are highly recommended at the energized high voltage end even for system voltages lesser than 500 kV.

4.3.7 Error Checks

The following checks were carried out in order to make sure that the simulations were accurate:

- All the assumptions and simplifications are made keeping the error factor lesser than 5%. To compute the error, the plot of electric field magnitude along the length of the insulator geometry was obtained and vector integration was performed on it with respect to displacement. The value thus obtained should be equal to the applied voltage. The difference between the applied voltage and the voltage thus calculated gives the error. Care was taken to keep this value less than 5% for all the cases.
- Secondly, the change in electric field calculations should not vary by a very large margin by changing the number of assigned elements.
- The tangential component of the electric field along the boundary of the insulator must be equal both inside and outside the insulator [9].
- The normal component of the electric field along a material boundary should be in inverse proportion to the dielectric constant of the two materials.

4.4 Electric Field Analysis under Wet Conditions

Composite insulators, made from polymer material with hydrophobic surfaces, have discrete water droplets on their surfaces under moist conditions (rain, fog etc) as against a thin film of water on porcelain material. A water droplet plays a number of roles in the electrical breakdown of air and insulating material junction. It not only enhances the electrical stress due to its high permittivity but also undergoes deformation in the presence of an electric field. The elongation of water droplet by electrostatic forces results in immediate increase in electric field at the drop tip, causing corona. It also behaves as a good conductor in the presence of contamination caused due to pollution and hence shorts out some of the insulating surface of the equipment, which might lead to pollution flashover. Therefore, it is very essential to analyze the effect of these droplets on the surface of the composite insulators

4.4.1 Insulator Geometry

For the work done here, water droplets are considered only along the surface of the sheath. Weather sheds are ignored to reduce complexity of the model and also computation time. It has been shown that the critical value of electric field for corona onset is lower for sheath region when compared to that of shed [11]. This justifies the consideration of water droplets only along the sheath region which is more prone to corona related to water droplets. The schematic of a 30 ° section of a 138 kV composite insulator under wet conditions is shown in Figure 10. The diameter of water droplets and the separation between them is taken as 6 mm. A perfectly hydrophobic material makes a contact angle of 90° with the surface. The electric field is plotted along a line though the junction of the water-air-insulating material along the length of the insulator.

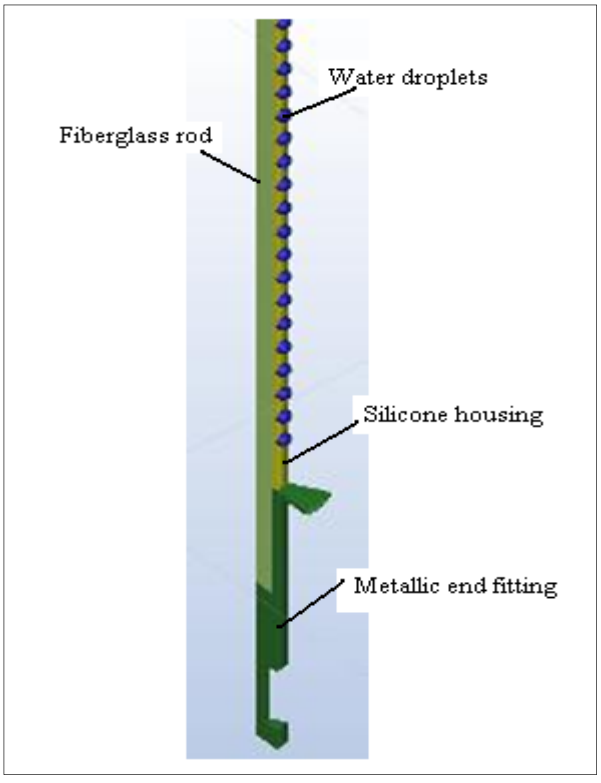

Figure 10. Schematic of a 30 ° section of a 138 kV composite insulator under wet conditions modeled in COULOMB

4.4.2 Assigning Physical Conditions

Relative permittivity of 80 is considered for water droplets, while the conductivity is set at 20 μS/cm. The boundary conditions are the same as that for dry case.

4.4.3 Assigning Boundary Elements

For wet conditions, the distribution of boundary elements is not uniform. Elements are assigned locally to each individual surface. Each water droplet is assigned 15 elements locally. System voltages for which a 30 degree section is modeled has twelve water droplets evenly distributed along the circumference. For 20° sections this number is eighteen. Table 4.4 in section 4.3.4 shows the total number of boundary elements assigned in case of each of the composite insulators modeled.

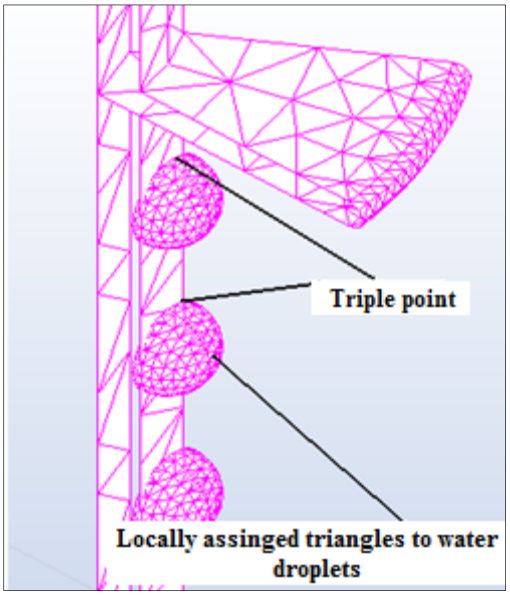

Figure 11. Boundary elements assigned locally to the water droplets under wet conditions

4.4.4 Electric Field Analysis for Wet Case

Electric field distribution along 230 kV and 1000 kV composite insulators under wet conditions are shown in Figure12 and 13 respectively. The electric field spikes at the water droplet – air – silicone sheath interface. The minimum electric field required for initiating streamer propagation in air varies from 0.45-1.1 kV/mm [12], [13].The lower value corresponds to positive polar-

ity and the higher value to negative polarity. For the purpose of this research, a value of 0.8 kV/mm is considered as the threshold for streamer propagation for electric field calculations under wet conditions.

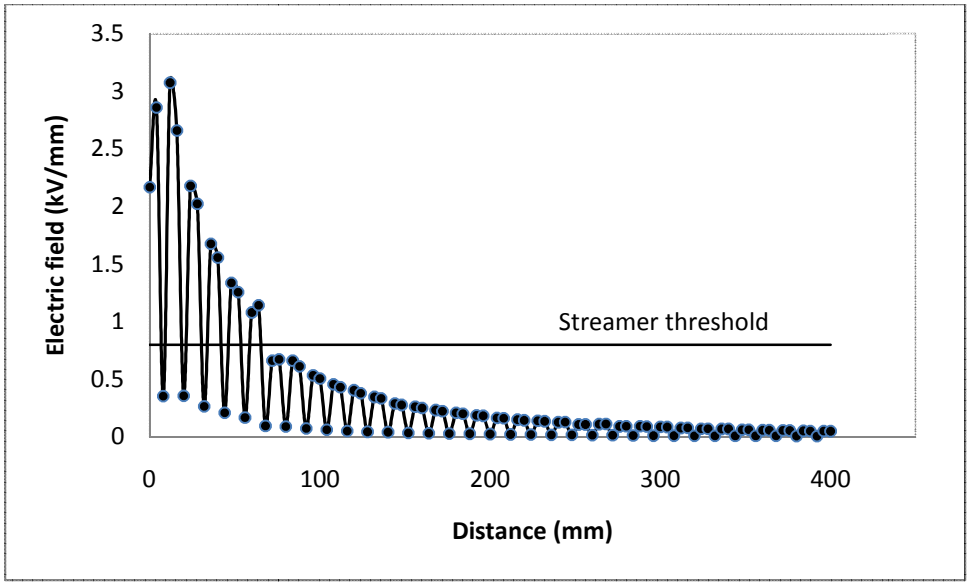

Figure 12. The electric field along a 230 kV composite insulator under wet conditions

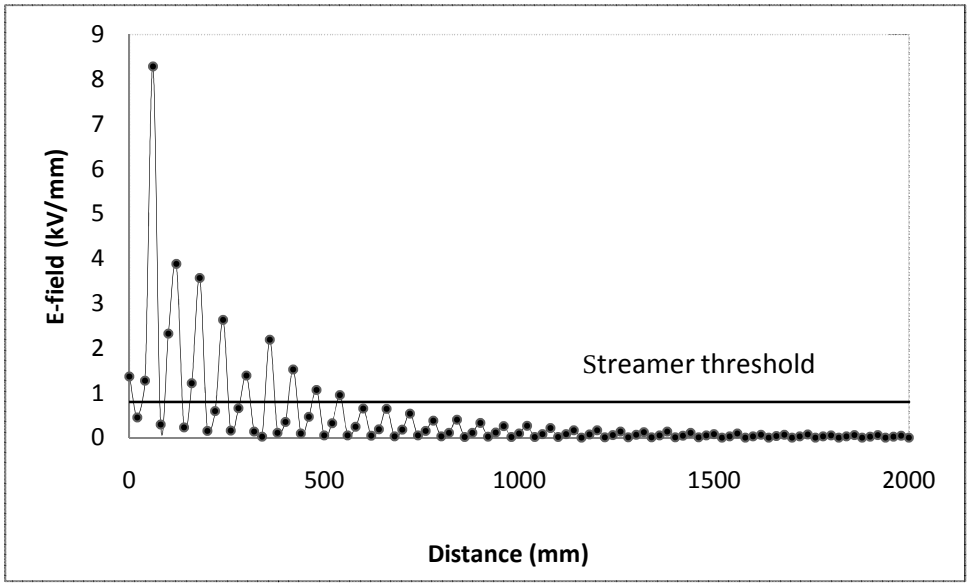

Figure 13. The electric field along a 1000 kV composite insulator under wet conditions

Figure 14 shows maximum electric field along composite insulators for different voltage ratings. It is concluded that the electric field enhancement is higher for higher voltage levels. In

order to prevent flashover by corona, it is essential to mitigate the high electric field which is located close to the energized end fitting and the rubber housing.

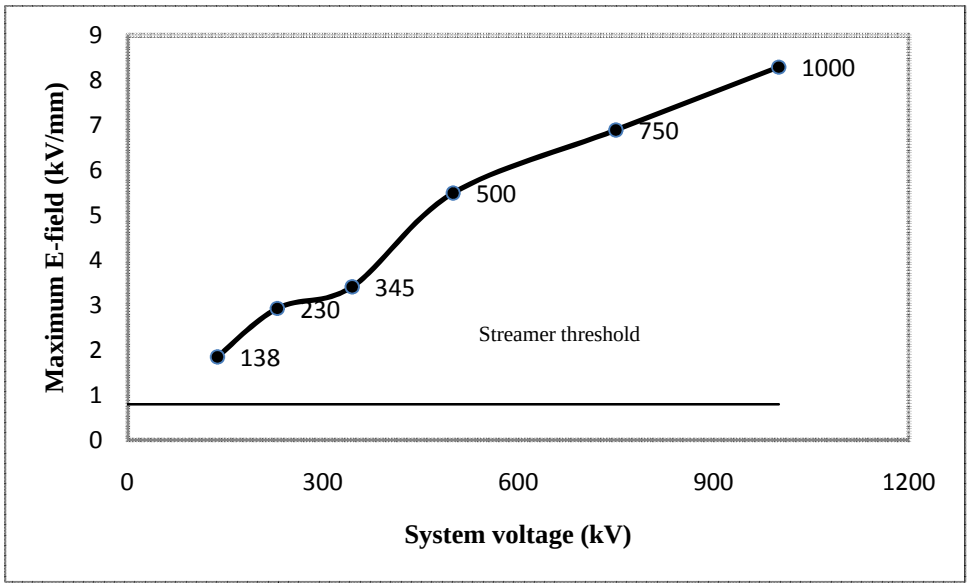

Figure 14. Maximum E – field as a function of system voltage under wet conditions

4.5 Effect of Addition of Corona Rings under Dry Conditions

In dry conditions, high electric fields might cause continuous corona activity on the metallic end fittings and insulator surface which is close to these end fittings. This might lead to erosion of the insulator surface and ultimately exposure of the fiberglass rod to the environment making it vulnerable to failure modes such as brittle fracture, partial discharge activity or an internal flashover. Calculations performed along the length of composite insulators under dry conditions showed that the maximum electric field occurred in the line side of the composite insulators. To suppress this field, corona rings of appropriate dimensions are added to the composite insulators modeled under dry conditions. Table 4.5 shows the dimensions of these rings. Figure 15 (a) and (b) show corona rings modeled with composite insulators for 230 kV and 345 kV composite insulators.

Table 4-5. Dimensions of corona rings used at different voltage ratings at line and grounded end

Voltage rating (kV)	Corona ring added		Ring diameter (inch)	
	Line-end	Grounded-end	Line-end	Grounded-end
138	No	No	-	-
230	Yes	No	8	-
345	Yes	Yes	15	8
500	Yes	Yes	15	15
765	Yes	Yes	15	15
1000	Yes	Yes	30	30
1200	Yes	Yes	30	30

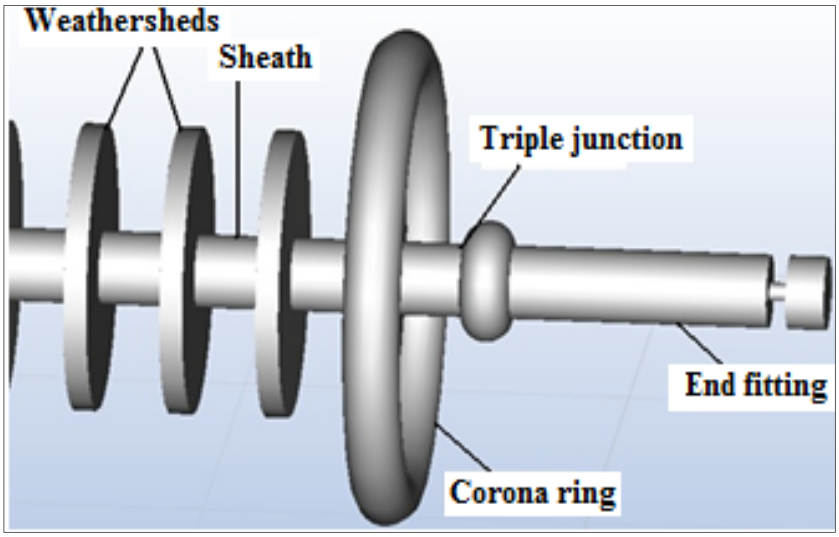

Figure 15. Schematic of corona rings around composite insulators in COULOMB

With the installation of corona rings, not only is the maximum electric stress area transferred from the sections between the end fittings and the first shed to the outer side of the ring, but the maximum electric field value is also reduced**.** Figure 16 shows a comparison between the maximum electric field values calculated along composite insulators at different voltage ratings with and without corona ring as a function of rated voltage.

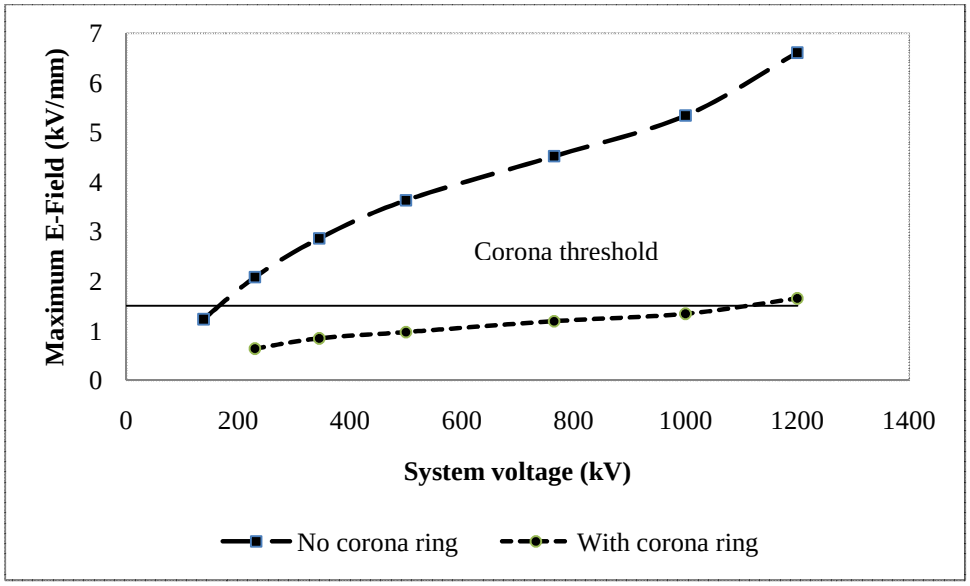

Figure 16. Maximum E-field as a function of system voltage under dry conditions considering the effect of corona rings

It is concluded from these results that the addition of corona rings mitigates the highest electric field to appreciable levels. Corona free operation can be expected for voltage rating up to 765 kV by proper application of rings. Corona rings are recommended even for lower system voltages like 230 kV and 234 kV in case of composite insulators. However, for UHV levels the electric field value is found to be on the higher side even after application of rings and therefore ring size and position optimization is performed for corona free operation which is discussed in the sections that follow.

4.6 Effect of Bundled Conductors on Electric Field along Composite Insulators

Generally EHV and UHV transmission systems employ the technique of bundled conductors which refers to having more than one conductor per phase. It not only improves the load carrying capacity of the transmission line but also helps in the reduction of high electric fields around the conductors. The work presented here contributes to the study of the effect of bundled conductors on electric field calculations along the surface of composite insulators. For EHV (500 kV and 765 kV) systems, cases with 1, 2, 4, 6 conductors per bundle are modeled. For UHV systems,

cases with, 1, 4, 6, 8, 10, 12 conductors per bundle are modeled. Regular intra bundle spacing of 18 inches is considered which is independent of line voltage, load carrying capacity and subconductors [14], [15]. Conductor diameter is taken as 1.165 inches. Corona rings of appropriate dimensions (as discussed in the previous section) are also considered along with the bundled conductors. For all cases, side down configuration of the bundles is considered. For instance, for a three conductor bundle, the base of the triangle formed by the three conductors would be parallel to the ground surface. Figure 17 (a) shows the schematic of a 500 kV composite insulator structure supporting a three bundled conductor configuration. Figure 17 (b) demonstrates the alignment of the three conductors in the bundle.

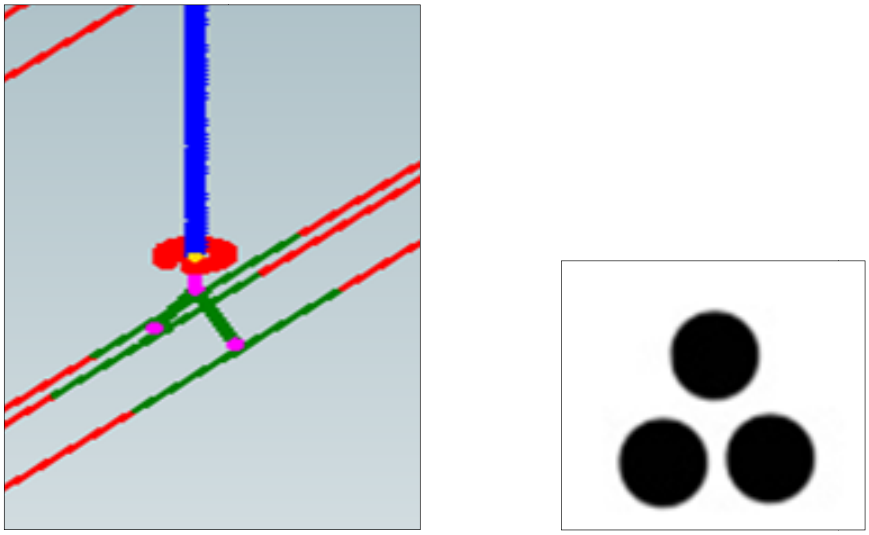

(a) (b)

Figure 17. Schematic of bundled conductors with side down configuration for a 500 kV voltage system (a) perspective view of the bundle and (b) demonstrating the alignment of the three conductors in the bundle

The relationship between the maximum electric field on the surface of the composite insulator versus the number of conductors per bundle for all voltage ratings is shown in Figure 18. According to this, the maximum field value along the surface of the composite insulators decreases appreciably as the number of conductors in a bundle is increased. There is a practi-

cal limitation on the number of conductors that can be used per bundle for different voltage ratings. Keeping that in mind, four conductors per bundle were used for EHV (5000 kV and 765 kV) systems and six for UHV (1000 kV and 12000 kV) systems.

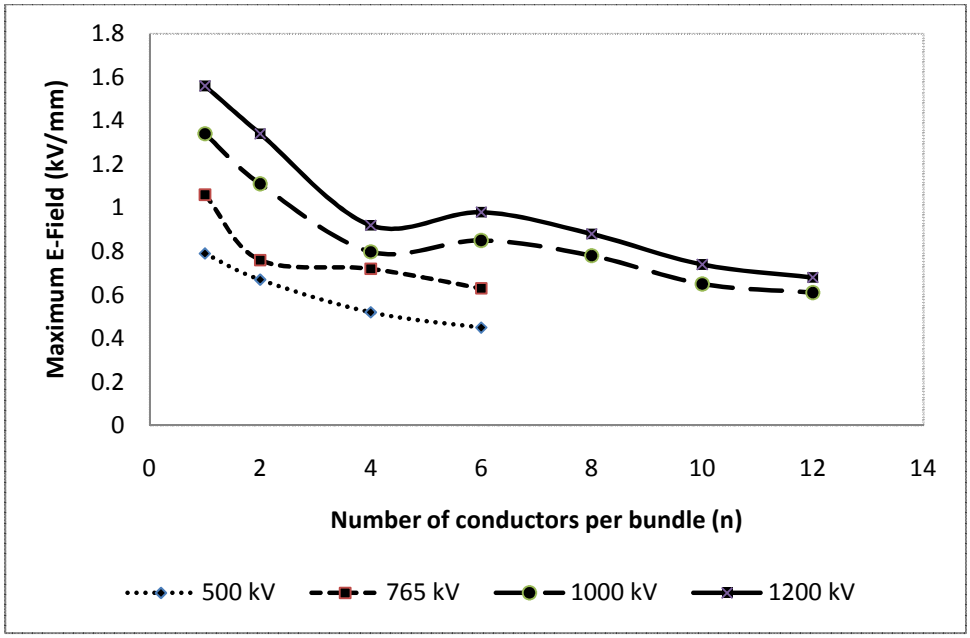

Figure 18. Maximum E-field as a function of number of conductors per bundle, considering the effect of corona rings, under dry conditions

The electric field calculations thus made were compared against the cases that considered only one conductor per bundle. The percentage decrease in the maximum E-field in these two cases is discussed in table 4-6. It is concluded that the effect of bundled conductors on the electric field along composite insulators in more prominent for higher system voltages.

Table 4-6. Effect of bundled conductors on E-field calculation of composite insulators under dry conditions.

Voltage rating (kV)	Maximum E-field (kV/mm)		Percentage decrease in maximum E-field
	N=1	N=4	
500	0.79	0.52	34%
765	1.06	0.72	32%
	N=1	N=6	
1000	1.34	0.85	37%
1200	1.56	0.89	43%

5. ANALYSIS OF UHV SYSTEMS

5.1 Introduction

Power generating and consumption sites are seldom in close vicinity. The bulk of electric power is transmitted through overhead lines from the generating sites to the distribution level. Most of these lines span over several thousands of kilometers. In order to minimize losses, power is transmitted at higher voltages in the order of several hundred kilovolts. UHV transmission systems not only transmit more power but also over vast distances with lesser transmission losses. Countries like The United States of America and Japan have systems over 700 kV ac that have been operating for many years now. Countries like China have recently installed 1000 kV transmission structures. Developing countries like India and Brazil are soon planning to venture into 1200 kV transmission systems. Gradually, there is a shift towards higher levels of voltages for the numerous advantages that they have [17]:

- An increase in the transmission capacity
- Reduced transmission losses (I^2R losses): large power transferred at low current value which implies lower transmission line losses
- Reduction in cost per unit transmission capacity: High amount of power can be transferred without installing multiple transmission lines and equipments
- Reduced land requirements
- Transmission over vast distances

Although, high voltages and currents, long distances and variable power flows of UHV transmission systems might make reactive power control more challenging in terms of requirement of appropriate reactive power compensation devices [16].

Higher voltages subject the composite insulators used to even higher electrical stress. In additions to that, non-linear electric field and voltage distribution along composite insulators used in UHV transmission systems is a major issue. This is attributed to the capacitive effects of conductors, tower and other hardware fittings. Non linearity is more severe in case of composite insu-

lators when compared to porcelain because of the absence of intermediate metal parts [18]. In addition to that, the electric field value close to the energized high voltage end is much above the threshold value under dry conditions without any mitigation technique, as shown in the previous chapter. This might lead to corona activity, partial discharge and premature aging of the insulator in use. Therefore, for reliable performance and long life of composite insulators used in UHV transmission systems, analysis of EFVD and finding ways to deal with the problem of non-linearity is of utmost importance and interest.

5.2 Grading Ring Optimization

Unfortunately, there exist no specific standards for the design and placement of grading rings. Each manufacturer makes independent recommendations for the use of their customized corona control rings [1]. It is therefore very important for the user to analyze their system and install appropriate rings. This sections presents optimization applied to design parameters for grading ring to be used for a 1000 kV system. The three principle variables considered for optimization are as shown in Figure 19:

i. The ring diameter (D)

ii. Diameter of the ring tube (T)

iii. Position of the ring from the energized high voltage end fitting (P)

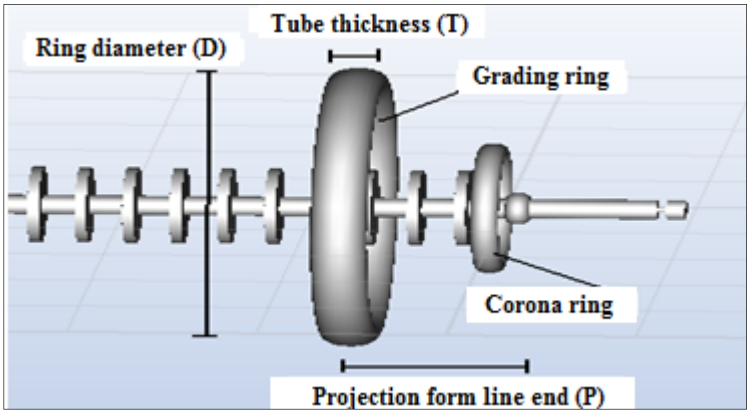

Figure 19. Schematic of parameters to be optimized for a grading ring to be installed on a 1000 kV composite insulator designed in COULOMB

The Electric field calculations are carried out for D, T, and P independently while keeping the other two constant. The parameters of the small ring in the high voltage part end are: ring diameter = 400 mm, ring tube thickness = 50 mm and distance of the ring from the energized end fitting is 0 mm. These parameters are kept constant while those of the large ring are varied for the purpose of optimization.

5.2.1 Electric Field as a Function of Ring Diameter (D)

The corona ring diameter is varied from 800 mm to 1400 mm and it is found that the maximum electric field value close to the energized end fitting decreases as the ring diameter increases. Therefore, an optimized value of 1000 mm is chosen as the diameter of the ring as the decrease in electric field on further increasing the ring diameter is not significant. Figure 20 shows the same.

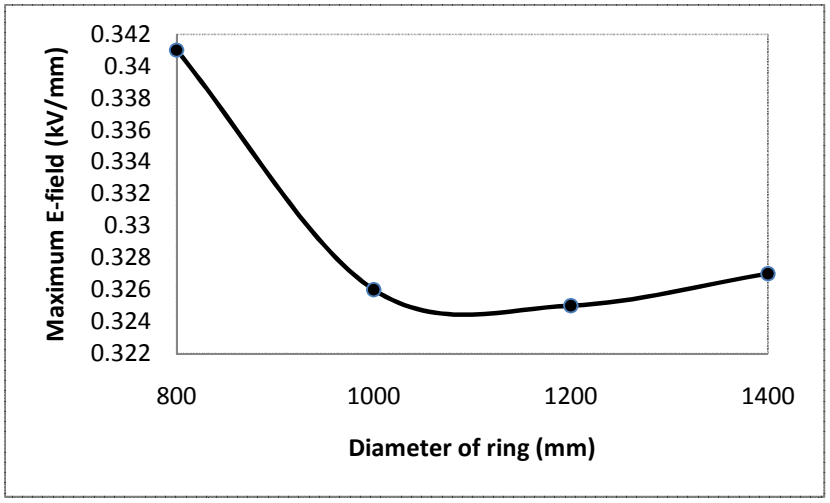

Figure 20. Effect of ring diameter D on maximum E-field along 1000 kV composite insulator

5.2.2 Electric Field as a Function of Ring Tube Diameter (T)

This section aims at analyzing the effect of the thickness of the corona ring tube on the electric field distribution along the composite insulator used in UHV transmission systems. The ring tube diameter is varied from 80 mm to 140 mm. Figure 21 shows the maximum electric field value along the surface of the composite insulator as the function of the ring tube thickness. The maximum field value decreases as the ring tube diameter is increases. The optimized parameter of

T is chosen to be 120 mm. Increasing T further only makes the ring more bulky whereas there is no significant decrease in the maximum electric field value.

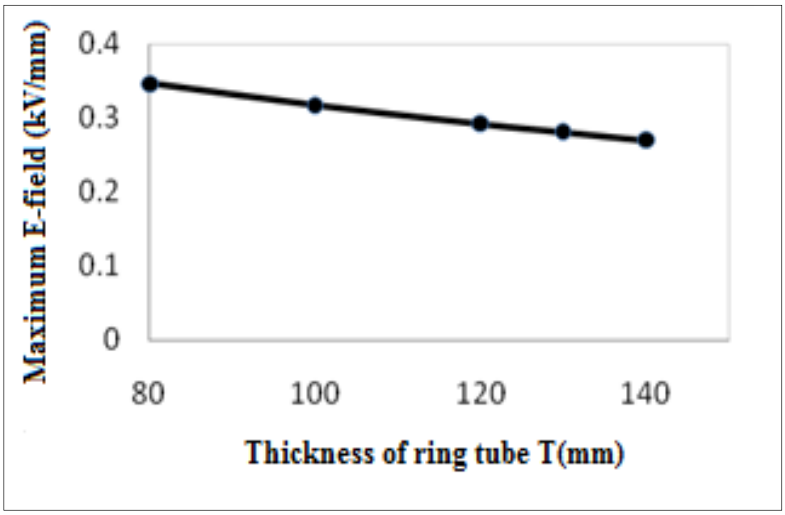

Figure 21. Effect of ring tube thickness T on maximum E-field along 1000 kV composite insulator

5.2.3 Electric Field as a Function of Position of the Ring from the Energized End Fitting (P)

The effect of placement of the corona ring with respect to the energized high voltage fitting is analyzed in this section. The position of the ring is changed from P = 0, which refers to the junction of the energized high voltage end fitting and the rubber sheath to P = 700 mm. As seen in figure 26, the maximum electric field value along the composite insulator at first decreases with the increase in the projection distance and then increases again. P is not varied beyond 700 as the dry arc distance decreases as P increases. Keeping that in mind, the optimized parameter of P is chosen to be 400 mm.

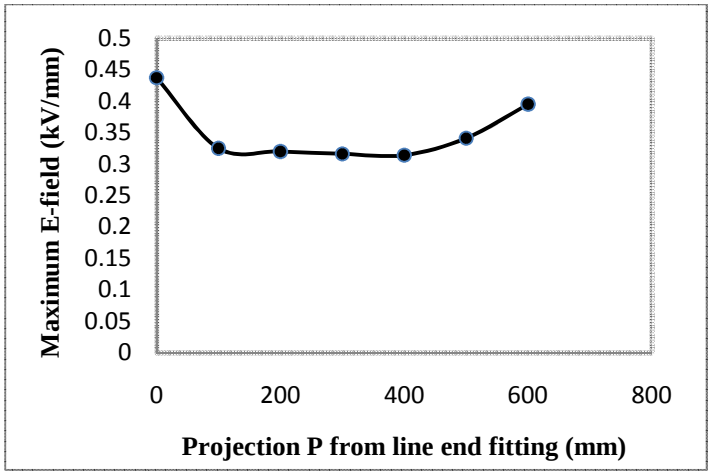

Figure 22. Effect of projection P from energized end fitting on maximum E-field along 1000 kV composite insulator

5.3 The Effect of Grading Ring on Double Units

On the 1000 kV line in operation, the use of two insulators per suspension string as shown in Fig 23 (for both I or V string) and up to 4 insulators per dead-end string is widespread. This is done for reliability reasons as if one insulator fails it will not cause the conductor to drop. In such cases, each insulator has its own corona ring at the line and ground end and a common grading ring at the line end. To evaluate the effectiveness of this arrangement, the electric field near the line end of the string was calculated and compared with single insulator string configurations shown in Figures 15 (corona rings only) and 19 (corona rings and grading ring at line end). For the double unit string a large grading ring of diameter 3200 mm (D) and ring tube diameter 140 mm (T) and placed at a distance of 400 mm (P) from the high voltage end fitting.

This section presents the effect of this grading ring on the electric field and voltage distribution along double string composite insulators especially employed in UHV transmission systems. Both the units of insulators have their individual corona rings on high voltage as well as grounded side. The parameters of this ring are: D = 400 mm, T = 50 mm and P = 0 mm. Bundled conductors with 6 conductors per bundle for both 1000 kV and 1200 kV are considered.

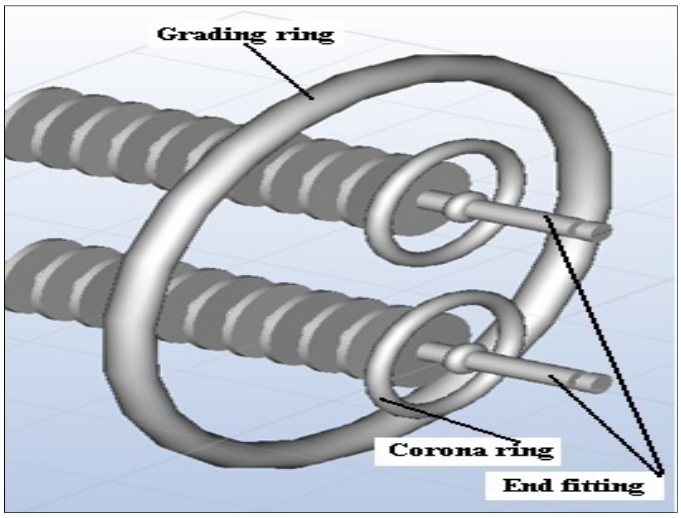

Figure 23. Schematic of grading ring applied to a 1000 kV UHV composite insulator in COULOMB

5.3.1 Results for 1000 kV UHV System

The effect of the grading ring is such that the electric field and voltage distribution along the 1000 kV composite insulator is improved to an acceptable level. The maximum electric field value is reduced to 0.508 kV/mm which is well under the corona inception threshold set at 1.5 kV/mm under dry conditions as evident from Figure 24. Figure 25 shows that the insulation distance, which bears 50% of the total applied voltage, is raised to be 1860 mm with the grading ring installed, while the distance without the grading ring is only 1150 mm: an increase by 61%. In other words, the electric field and voltage distribution is found to be more linear with the application of grading rings.

The results of the calculations, shown in Figure 24, indicate that the reduction in the maximum electric field at the triple junction provided by the double unit arrangement when compared to the single unit arrangements is quite significant. Of course the cost will increase, but in certain locations such elaborate arrangements may be required when using composite insulators.

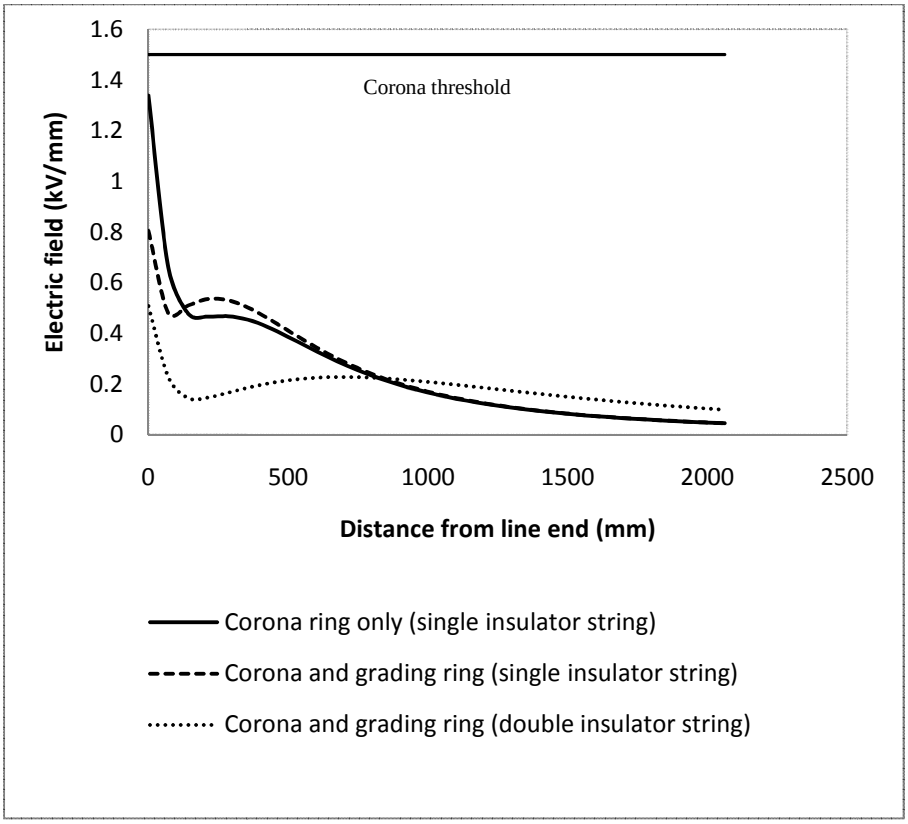

Figure 24. Electric field distribution along 1000 kV composite insulator with the addition of a grading ring

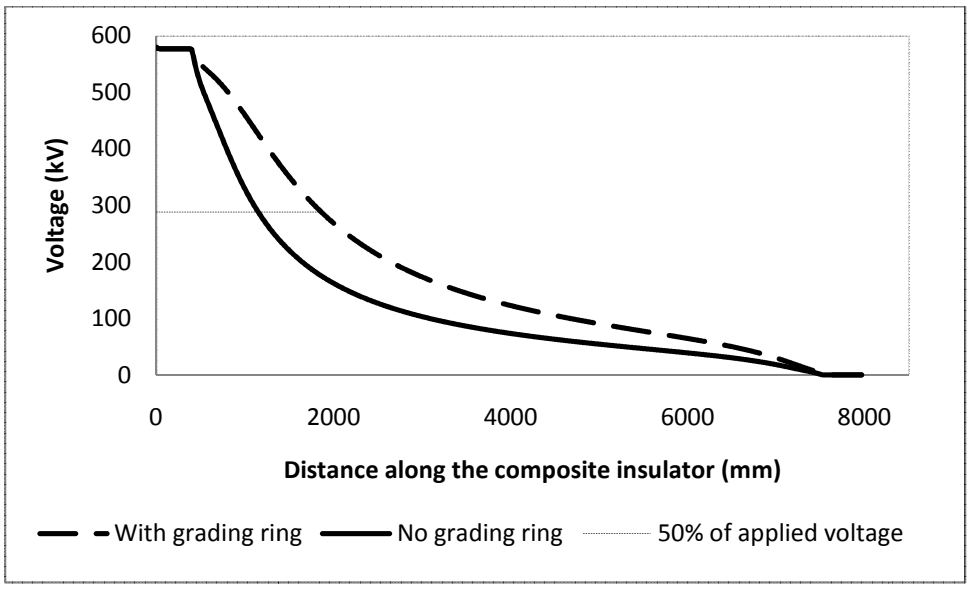

Figure 25. Potential distribution along 1000 kV composite insulator with and without grading ring

5.3.2 Results for 1200 kV UHV System

The effect of the grading ring on 1200 kV composite insulator is the same as that on the 1000 kV composite insulator. The maximum electric field value is reduced to 0.679 kV/mm which is well under the corona inception threshold set at 1.5 kV/mm under dry conditions. Figure 27 shows that the insulation distance, which bears 50% of the total applied voltage, is raised to be 1930 mm with the grading ring installed, while the distance without the grading ring is only 1040 mm. In other words, the electric field and voltage distribution is found to be more linear with the application of grading rings.

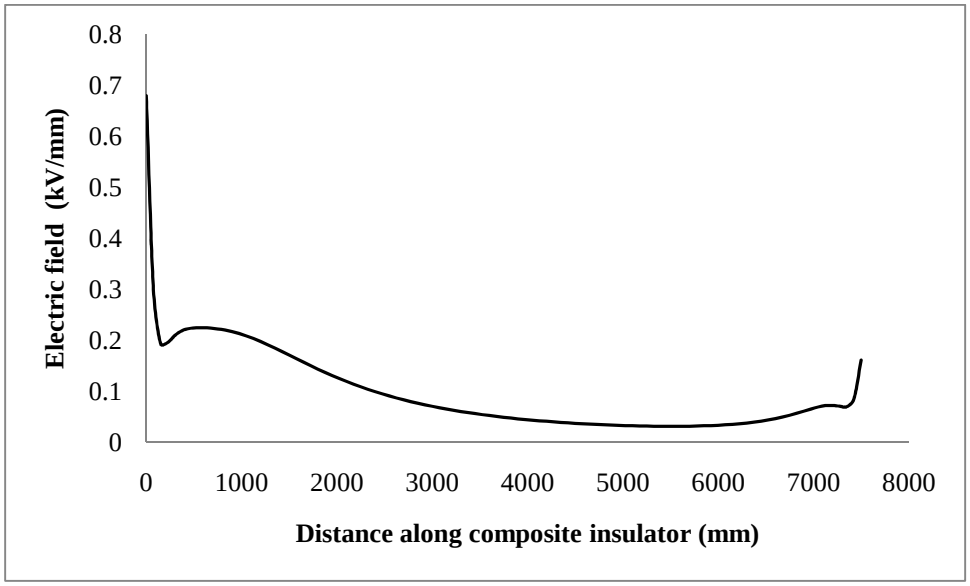

Figure 26. Electric field distribution along 1200 kV composite insulator with the addition of a grading ring

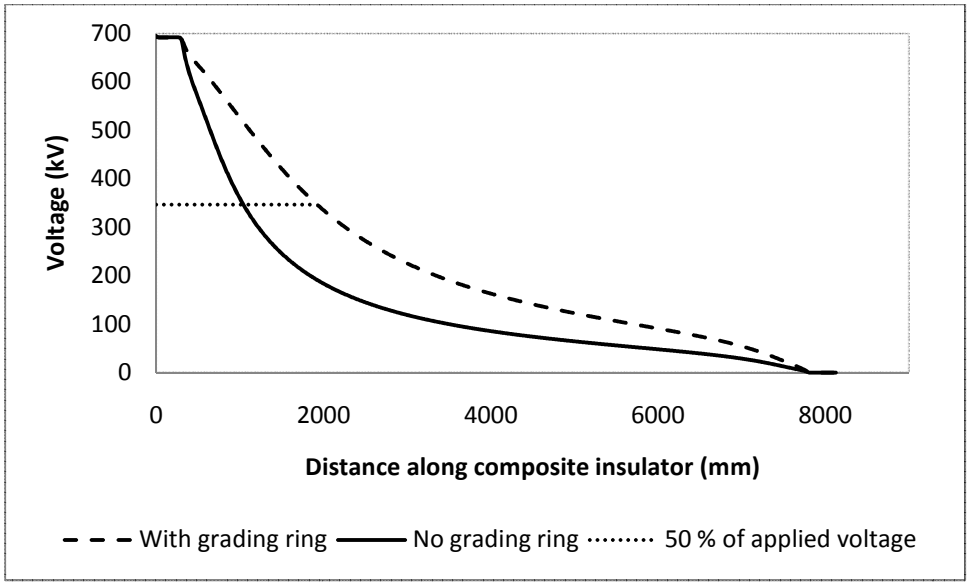

Figure 27. Potential distribution along 1200 kV composite insulator with and without grading ring

6. ELECTRIC FIELD ANALYSIS USING EPIC

6.1 Introduction

EPRI Software for Polymer Insulator Electric Field Calculations (EPIC) is developed for EPRI for the purpose of assessing polymer insulator performance. EPIC is, by large, used by utilities to make performance related analysis of the composite insulators installed or to be installed in the future on their power lines. The solver used in EPIC is based on the concept of Charge Simulation Method [19]. For the models constructed, all components from tower structure to the end fitting hardware can be selected from the vast database that the software provides. The component details are derived from the companies' catalogs that manufacture them. These can, however, be customized by the user as far as the dimensions are concerned. All simulations are carried out in a dry environment which basically considers the surface resistance to be infinite.

For the purpose of the work presented here, EPIC 3.1 Beta version was used on a workstation with the following specifications: Windows XP, 1.95 GB RAM and 2.99 GHz processor speed, 3D Graphics Video Card with OpenGL Drivers. The following sections give a brief description about the various tools provided by the software and their application in creating suspension and dead end models for the purpose of this research.

6.2 Modeling 138 kV Suspension Structure

A typical suspension structure supports the conductors vertically by a suspension insulator assembly. For the purpose of this research, a 138 kV suspension structure is modeled in EPIC software taking the entire geometry into consideration. This consists of the tower geometry, all three phases, phase conductors, ground wire, metal end fittings, structure attachment hardware, composite insulators and corona rings, if any. Single circuits are considered for the case of 138 kV rated suspension model. A systematic step by step procedure is followed to specify design characteristics of all the parts. Changes can be made to any one or more parts without disturbing the rest of the geometry, which is very convenient feature. In case of misfit of any part due of dimension constraints, an error message is displayed. Appropriate changes can be made to take care of that.

Minor co-ordinate misfits are automatically set right by the software. Following steps are taken in order to model the geometry:

6.2.1 Choosing Tower Configuration

The tower structure chosen for the 138 kV suspension structure is tubular or pole type. The structure is a standard model with the dimensions as shown in Figure 28 and is represented by the code name ‘STSIEEE’. The dimensions are specified in table 6-1. These can be customized.

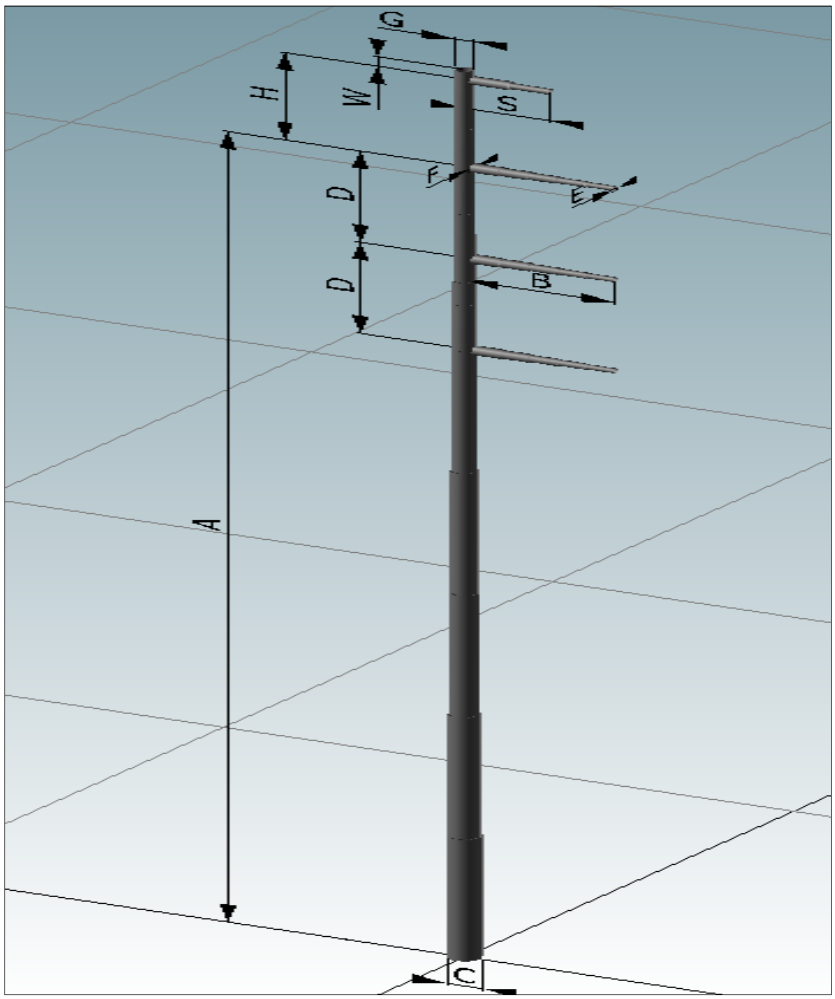

Figure 28. Tower configuration and dimension for 138 kV suspension model

Table 6-1 Tower dimensions for 138 kV suspension model

Segment	Segment length (mm)
A	27.150
B	2.650
C	0.600
D	3.130
E	0.140
F	0.310
G	0.300
H	3.000
S	1.500
W	0.330

6.2.2 Phase and Ground Wire Specifications

Line to ground voltage of the system is specified as 79.67 kV, which is the line voltage divided by square root of three. ACSR Drake conductors are used for phase wires with diameter equal to 28.1 mm while 7/16 HS with diameter equal to 11 mm is used for ground wire. One conductor per bundle is considered for phase wires. The co-ordinates for the phase and ground wire are set as shown in Figure 29.

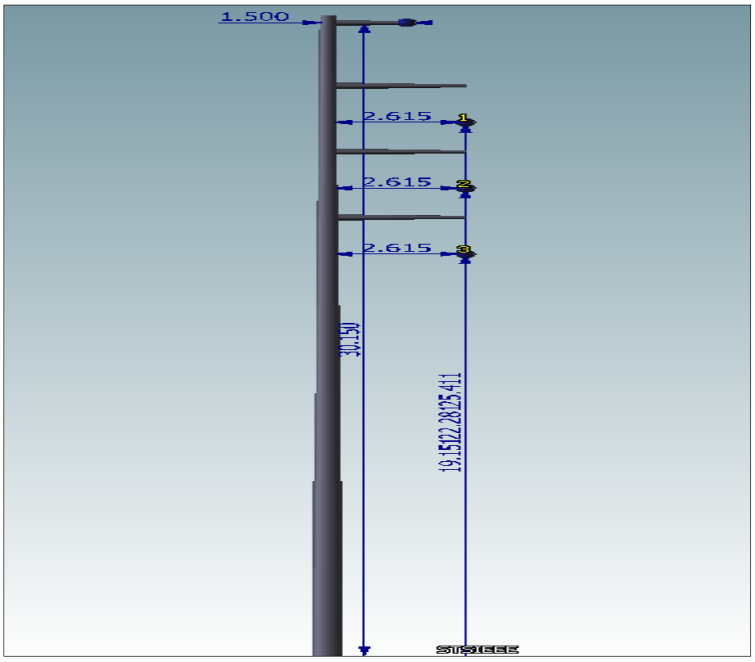

Figure 29. Phase and ground wire co-ordinates for 138 kV suspension model

6.2.3 Attachment and Hardware Specifications

The attachment hardware part numbers are chosen as specified by EPRI Task Force on modeling of composite insulators [6]. Figure 30 shows a basic layout of the various parts used. The catalog names of these parts are mentioned in Table 6-2.

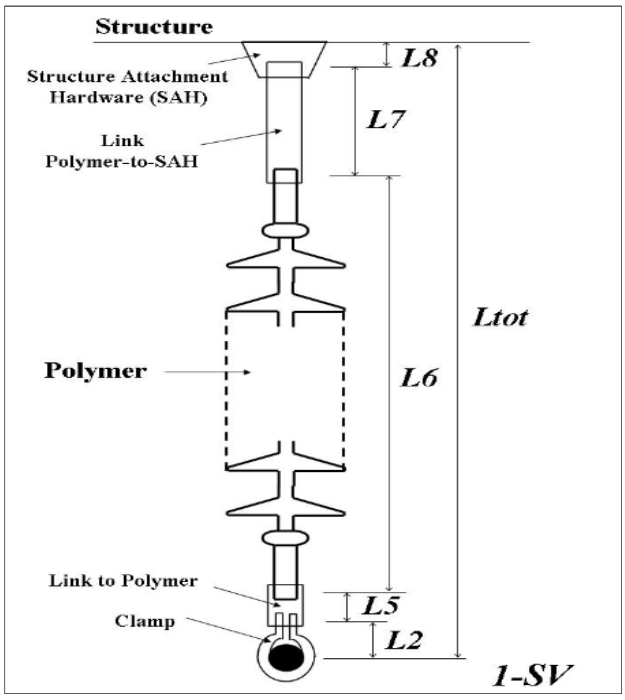

Figure 30. Attachment hardware layout for 138 kV suspension insulator

Table 6-2 Attachment hardware specifications for 138 kV suspension insulator

Designation	Product catalog number
L2 - Clamp	# HAS -139-S
L5 – Link to Polymer	# SA-13
L – 7 Link Polymer to Structure Attachment Hardware	None
L8 - Structure Attachment Hardware (SAH) Catalog # SAH-P-Custom-3	# SAH-P-Custom-3

6.2.4 Composite Insulator and End Fittings Specifications

The composite insulator modeled is according to the IEEE standard model in EPIC. The other specifications are as in Table 6-3.

Table 6-3 Composite insulator geometry and material properties for 138 kV suspension insulator

Connection length	1316 mm
Leakage distance	2806 mm
Energized end hardware	Ball
Grounded end hardware	Y – clevis
End fittings material	Galvanized steel
Rubber material	Relative permittivity = 4
Fiberglass rod	Relative permittivity = 5.5
Insulator Type	Hi*Lite
Standard Mechanical Load (SML)	25/30 KIP

6.2.5 Determination of the Worst Affected Phase

Initial runs are made to determine the phase that undergoes the highest electrical stress among all three. Electric field measurements are made along the composite insulators at various locations on all three phases of the 138 kV suspension model. It is observed that the middle phase is the worst affected and the electric field values are the maximum along insulators in the middle phase. For instance, the electric field magnitudes in phases A and C are found to be 6% and 5% less than that in phase B for calculations along the surface of the composite insulator from the energized end fitting.

6.2.6 Electric Field Calculations for 138 kV Suspension Structure

Figure 31 shows the complete model designed for a 138 kV suspension structure in EPIC 3.1 Beta software.

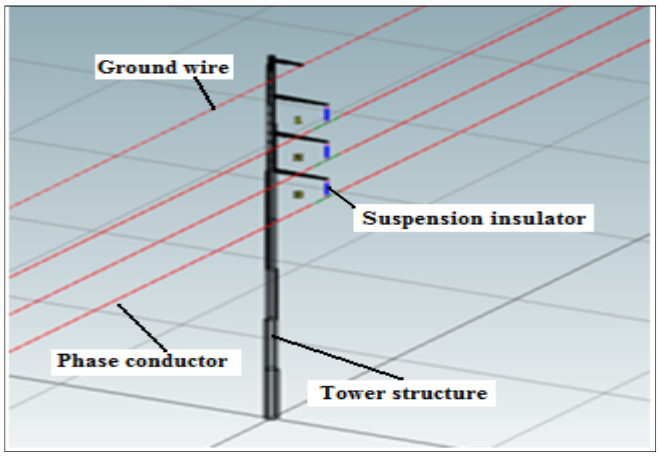

Figure 31. 138 kV suspension structure modeled in EPIC 3.1 Beta

For electric field calculations, measurements are made along five different locations as recommended by EPRI [6]. All measurements are made along the middle phase composite insulator as it is established that the maximum field values occur in the middle phase insulator in the previous section:

I. Electric Field magnitude along the surface of the rubber sheath of the middle phase composite insulator. Measurement is made for a distance of 300 (along C) mm, starting 1 mm from the energized end fitting, marked by B. The line of measurement is 1 mm above the surface of the insulator marked by D. It is ensured that the line of measurement is straight and parallel to the axis of the insulator as shown in Figure 32.

II. Electric field magnitude along the surface of the rubber sheath from the grounded end fitting. Measurement line is the same as above.

III. Electric field magnitude along the fiberglass rod from energized end fitting. Measurement line is the same as case I.

IV. Electric field magnitude along the energized end fitting.

V. Electric field measurement along the grounded end fitting.

The Figure 33-35 and Figure 37-38 show the graphical results for the above cases.

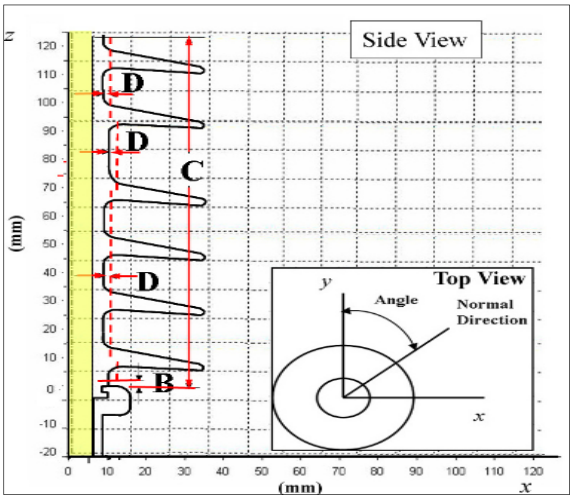

Figure 32. Figure showing the line of measurement along the surface of the rubber sheath of a 138 kV suspension insulator

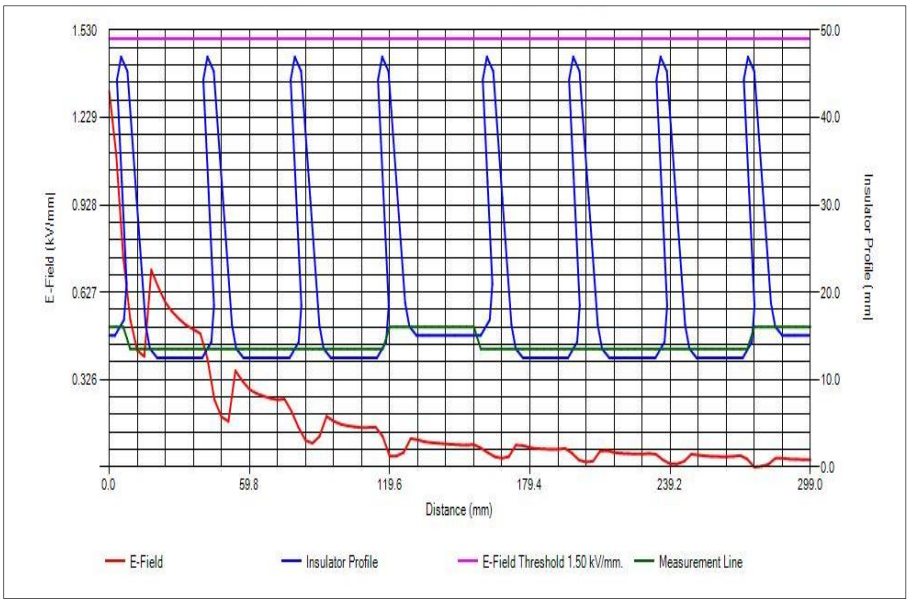

Figure 33. Electric field along the insulator rubber sheath from the energized end fitting for a 138 kV suspension model- case I

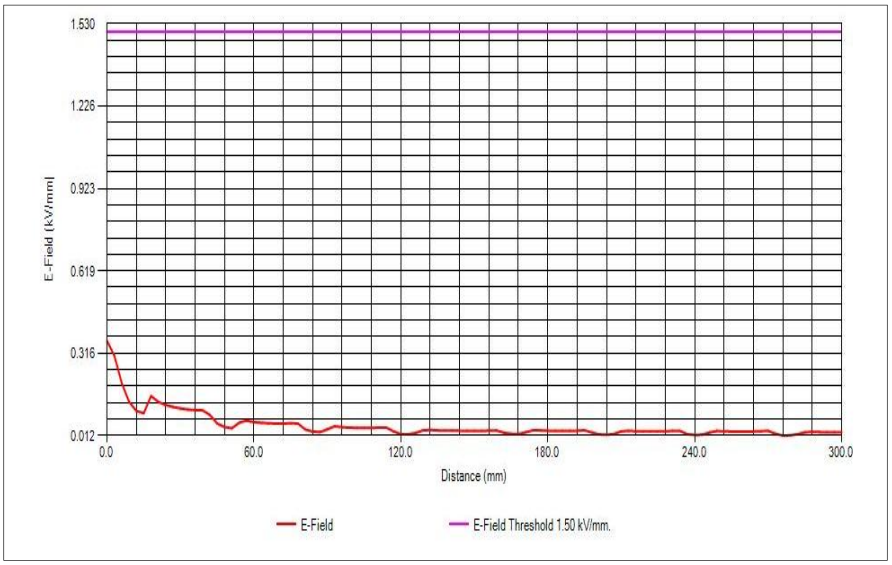

Figure 34. Electric field along the insulator sheath from the grounded end fitting 138 kV suspension model- case II

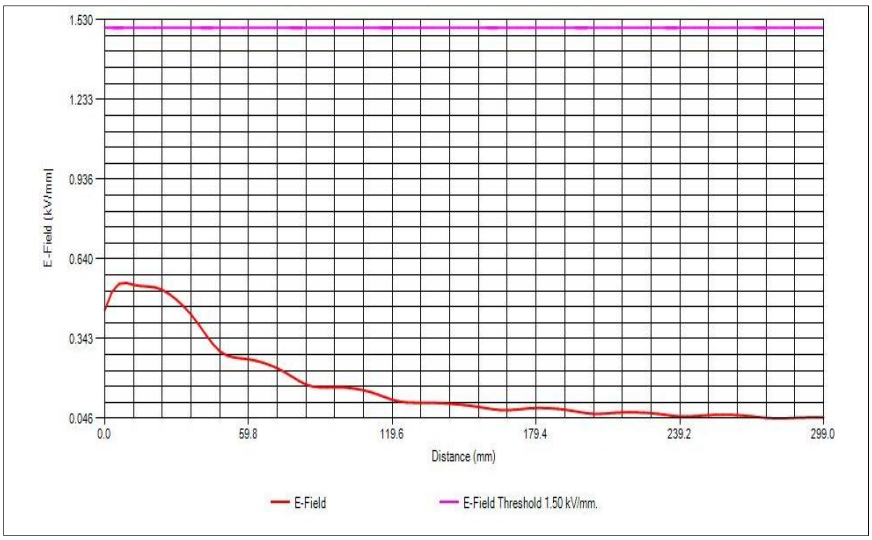

Figure 35. Electric field along the fiberglass rod from the energized end fitting for a 138 kV suspension model- case III

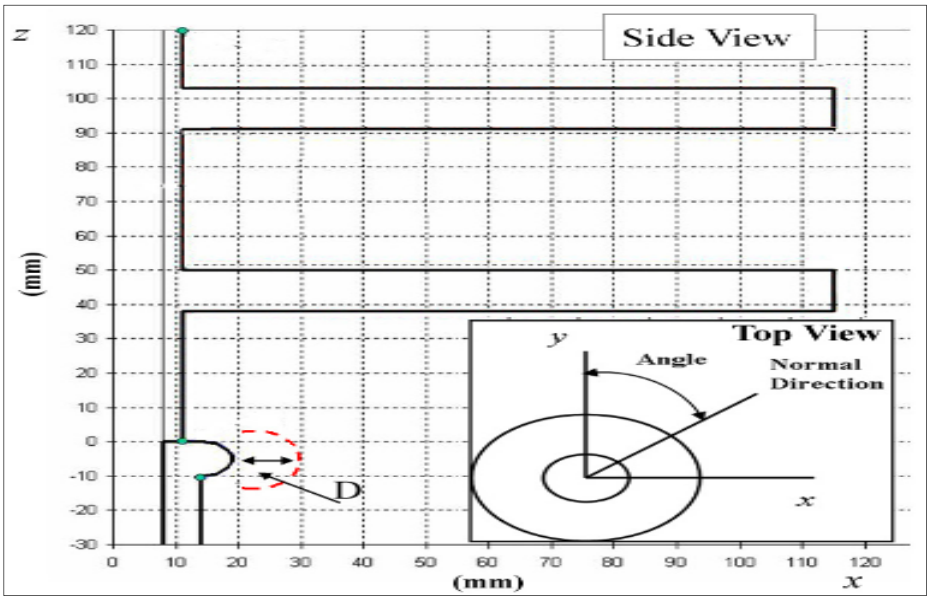

Figure 36. Line of measurement along end fitting of the insulator for a 138 kV suspension model

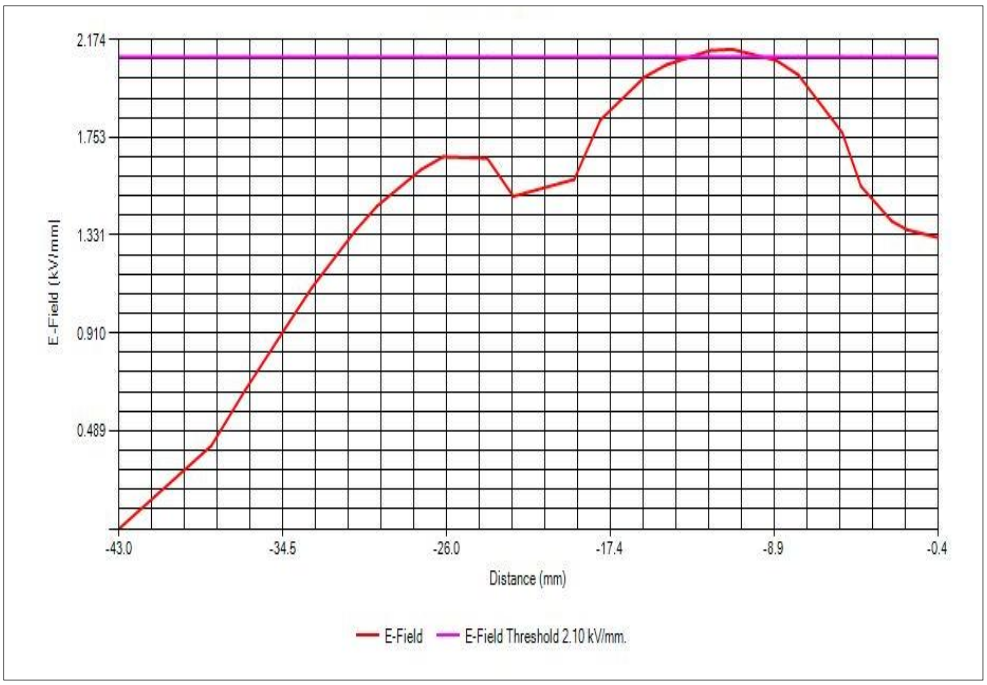

Figure 37. Electric field along the energized end fitting for a 138 kV suspension model

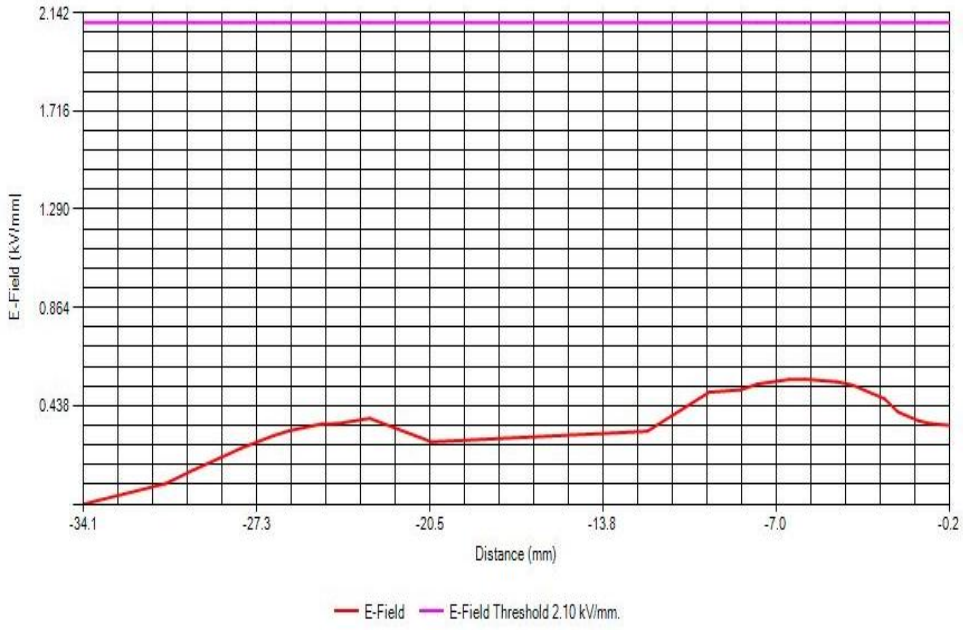

Figure 38. Electric field along the grounded end fitting for a 138 kV suspension model

Table 6-4 summarized the maximum electric field values and their location for all five cases as seen in the graphs above. The locations for cases I, II and III refer to the distance away from the junction of the end fitting and the rubber sheath towards the length of the insulator. Those for cases IV and V refer to the distance away from the junction of the end fitting and the rubber sheath towards the length of the end fitting. A value of 1.5 kV/mm is set at the threshold for corona initiation.

Table 6-4 Maximum electric field values and their location along 138 kV suspension insulator

	Maximum electric field (kV/mm)	Location of this field (mm)
I.	1.32	1 mm
II.	0.36	At the junction of grounded end fitting and sheath
III.	0.55	8.9 mm
IV.	2.13	11.09 mm
V.	0.55	5.85 mm

6.3 Modeling 138 kV Dead End Structure

Dead end structures are used where the transmission line either ends to follow a substation or when it turns through a large angle. The insulator string is in line with the conductor and under tension. This section presents modeling of a 138 kV dead end structure and evaluation of the performance of composite insulators supporting the conductors with the help of electric field calculations. A comparison is made to the electric field calculations carried out for suspension model of the same voltage rating. The steps that are followed are more or less that same as those for suspension model. There are a few changes that are incorporated in this design which are discussed in the sections that follow. Single circuit is considered for this model. Figure 39 shows a pictorial representation of the modeled dead end structure in EPIC software.

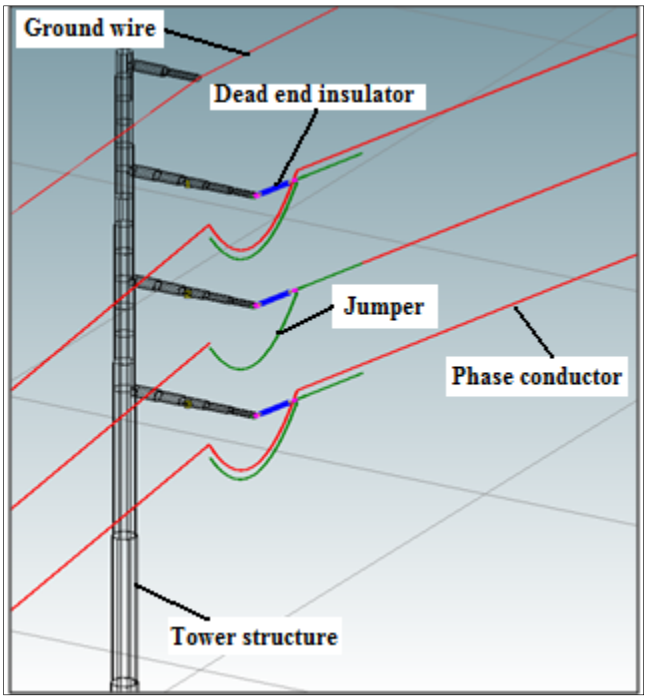

Figure 39. 138 kV dead end structure modeled in EPIC 3.1 Beta

6.3.1 Tower Configuration, Phase and Ground Wire Specifications

The tower configuration chosen for 138 kV dead end structure is the same as that for suspension. The model code is STSIEEE. ACSR Drake conductors are used for phase wires with diameter equal to 28.1 mm while 7/16 HS with diameter equal to 11 mm is used for ground wire. One conductor per bundle is considered for phase wires.

6.3.2 Attachment and Hardware Specifications

The attachment hardware part numbers are chosen as specified by EPRI Task Force on modeling of composite insulators for dead end structures [6]. Figure 40 shows a basic layout of the various parts used. The catalog names of these parts are mentioned in Table 6-5.

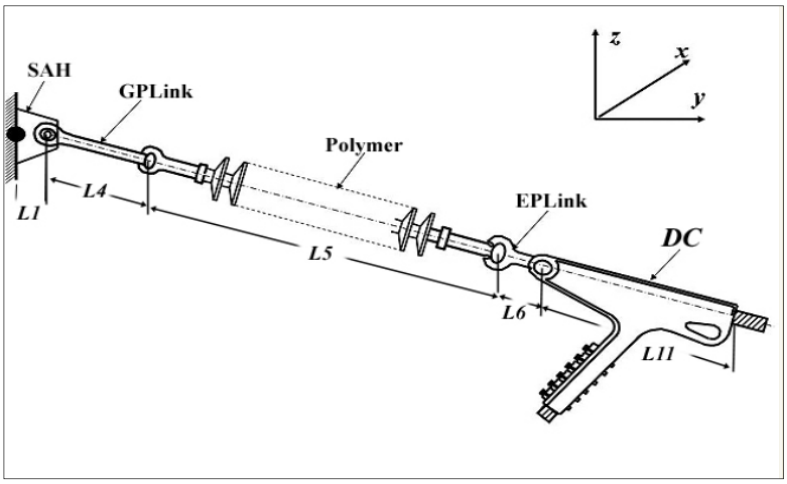

Figure 40. Attachment hardware specifications for 138 kV dead end insulator

Table 6-5 Specification of attachment hardware for 138 kV dead end insulator

Designation	Product catalog number
L1 – Structure Attachment Hardware (SAH)	#SAHD HP-Custom-2
L4 – Grounded Link to Polymer (GPLink)	None
L5 – Composite Insulator	IEEE
L6 - Energized Link to Polymer (EPLink)	#SYCS-30-90
L11- Dead End connector	#CDE -A0311

6.3.3 Composite Insulator and End Fittings Specifications

The insulator modeled is according to the IEEE standard model defined in EPIC. The material specifications and end fitting details are given in Table 6-6.

Table 6-6 Composite insulator geometry and material properties for 138 kV dead end insulator

Connection length	1316 mm
Leakage distance	2806 mm
Energized end hardware	Ball
Grounded end hardware	Y – clevis
End fittings material	Galvanized steel
Rubber material	Relative permittivity = 4
Fiberglass rod	Relative permittivity = 5.5
Insulator Type	Hi*Lite
Standard Mechanical Load (SML)	25/30 KIP

6.3.4 Electric Field Calculations for 138 kV Dead End Structure

The electric field calculations were made along the same five locations as for the suspension model. For the ease of representation, tabular structure is adopted here. Table 6-6 summarizes the maximum electric fields calculated along different locations along the composite insulator:

Table 6-7 Electric field results for 138 kV dead end composite insulator

	Maximum electric field (kV/mm)	Location of this field (mm)
I.	1.45	1 mm away from energized end fitting
II.	0.33	1 mm away from grounded end fitting
III.	0.87	6.6 mm away from energized end fitting
IV.	2.54	9.8 mm
V.	0.55	8.9 mm

6.4 Comparison of Electric Stress along Composite Insulators in Suspension and Dead End Environment for 138 kV System

Suspension structures support the conductors vertically with the help of a suspension insulator assembly whereas dead end structures support the conductors such that they are in line with the insulator string. The insulator string is in permanent tension which is unbalanced in nature. The purpose of modeling 138 kV rated system in dead end and suspension environments is to study the effect of this configuration on the performance of the composite insulators with the help of electric field calculations.

Electric field calculations carried out in EPIC software have shown that the maximum electric field stress calculated along composite insulators in dead end configuration is around 11 % higher when compared to its suspension counterpart, which is significant. Therefore, it is concluded that dead end insulators have higher electric field magnitudes when compared to suspension. Figure 41 shows the electric field distribution along the surface of the rubber sheath for 138 kV dead end and suspension insulators.

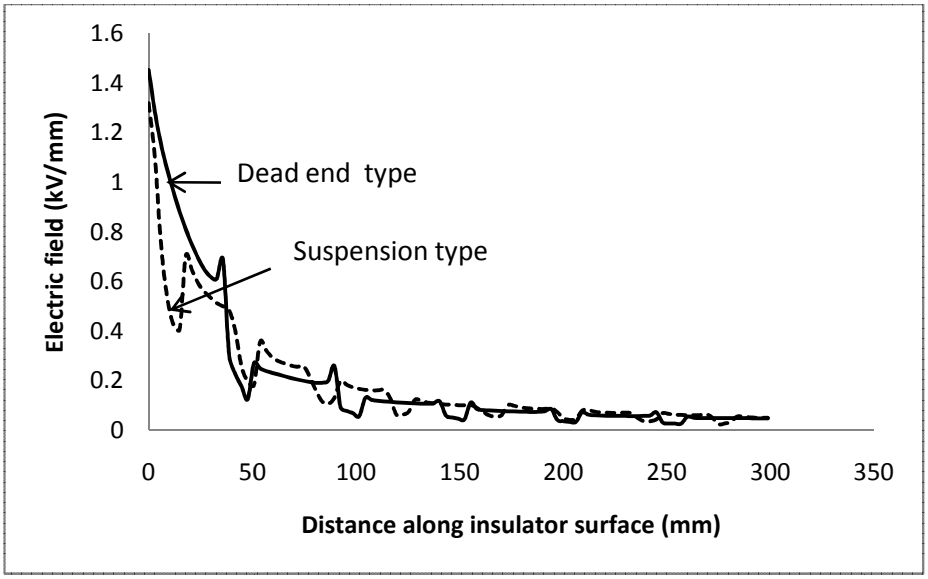

Figure 41. Comparison between electric field calculations of 138 kV dead end and suspension structure

The maximum value of electric field is found to occur very close to the junction of the rubber sheath and the metallic energized end fitting. This could lead to discharges and corona related activity which could expose the fiberglass rod to the environment and moisture. Degradation of the fiberglass rod or the polymer material of the composite insulator could lead to premature aging of the sample or deterioration in mechanical strength of the insulator. In order to mitigate this high electric field, a corona ring with diameter equal to 8 inches is recommended at the energized high voltage end. It is found that the application of this ring has reduced the maximum electric field value by around 76 % in case of the dead end model.

6.5 Comparison of Electric Stress along Composite Insulators in Suspension and Dead End Environment for dfferent Voltage Ratings

The electric field calculations made above are repeated for structures with higher voltage ratings. For ease in comparison, all models are considered without any corona ring. The models, both suspension and dead end, for voltage ratings 138 kV, 230 kV and 345 kV consider one conductor per bundle. For 500 kV systems, two conductors per bundle are considered. (This explains why the maximum electric field along the surface of the insulator for 500 kV is lesser than that of

345 kV. All these models are considered under dry conditions). All models consider single circuit configuration. The results obtained after electric field calculations along the surface of the composite insulators from the energized end fitting for both suspension and dead end structures for four different voltage ratings are documented in Table 6-8.

Table 6-8 Comparison of maximum electric field values along suspension and dead end composite insulators for different voltage ratings

Voltage rating (kV)	Maximum E-field along surface of insulator (kV/mm)		Percentage difference in E -field
	Suspension model	Dead end model	
138	1.32	1.45	11 %
230	2.21	2.63	19%
345	2.65	3.35	26%
500	2.50	3.24	30%

From the results above, it is concluded that:

- The maximum electric field value along the surface of composite insulator increases with the voltage rating of the system.
- The percentage difference between maximum electric field along suspension and dead end insulators increases as the voltage rating of the system goes higher.

The percentage difference in the maximum electric field values for suspension and dead end insulators as a function system voltage is shown in figure 42.

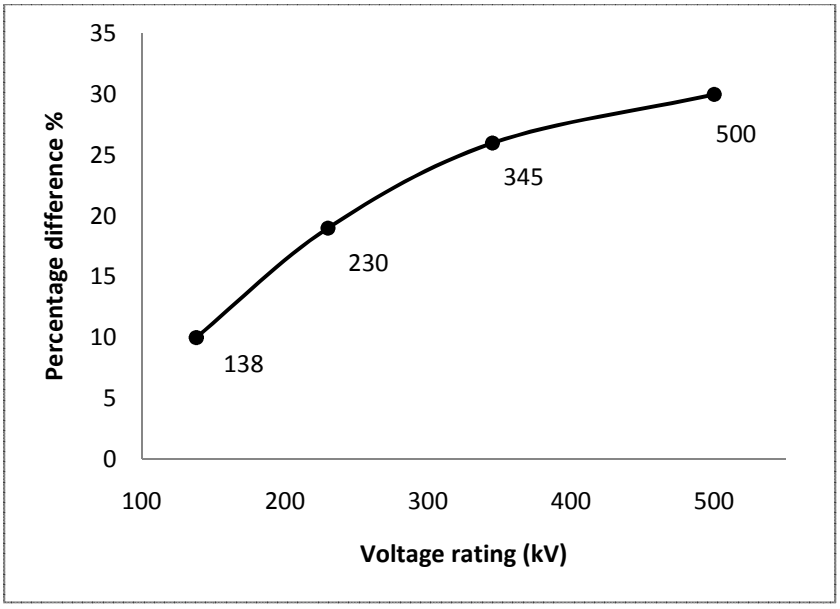

Figure 42. Percentage difference in maximum electric field between suspension and dead end insulators as a function of system voltage

6.6 Comparison between 230 kV Single and Double Circuit Dead End Structures

A single circuit transmission line carries one circuit consisting of three phases and appropriate ground wires whereas a double circuit line carries two circuits consisting of three phases each, on either side. This section presents the effect of the number of circuits on a transmission tower on the performance of the composite insulators used in these designs with the help of electric field calculations.

Single and double circuit 230 kV dead end structures are considered here for the purpose of analysis. The specifications of the entire geometry including tower structure, phase wire conductors, ground wires and hardware attachment structures are documented in Appendix C. One conductor per bundle is considered for both the cases. No corona mitigation technique is employed. The details of the composite insulator modeled are presented in Table 6-9. Figure 43 shows the modeled composite insulator in EPIC.

Table 6-9 Dimensions of 230 kV composite insulator for single and double circuit dead end structure

Manufacturer	Hubbell Power Systems
Insulator type	Hi*Lite
Catalog#	511012
SML	25/30 kip
Energized end fitting	Ball
Grounded end fitting	Eye
Base connection length	2121 mm
Leakage distance	4674 mm
Shed type	Regular
Number of sheds	48

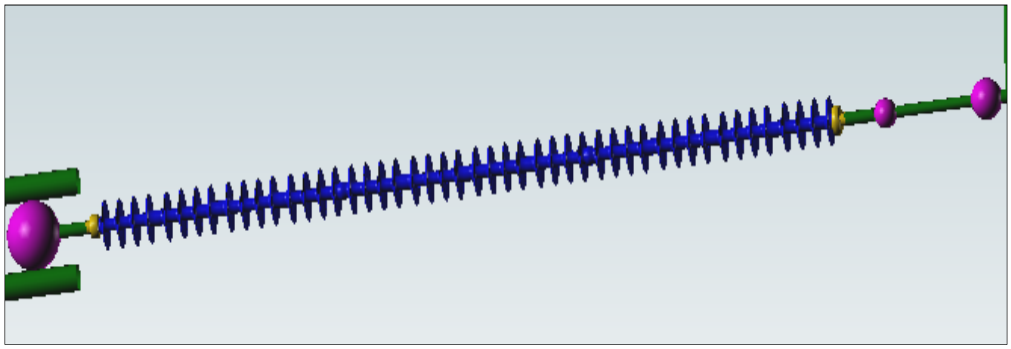

Figure 43. 230 kV modeled composite insulator for single circuit dead end structure

Figure 44 shows the electric field distribution along the surface of the composite insulators for a length of 120 mm, starting 1 mm from the energized high voltage end fitting. It can be seen that the maximum electric field value for single circuit dead end structure is18 % higher than that of double circuit dead end structure. This is a significance difference considering the fact that most of the other geometries related to both the structures are more or less the same. Therefore, appropriate measures should be taken to mitigate this high electric field. For instance, application of a corona ring with diameter equal to 8 inches at the high voltage end fitting for single circuit dead end structure leads to reduction in the maximum field value by 65 %.

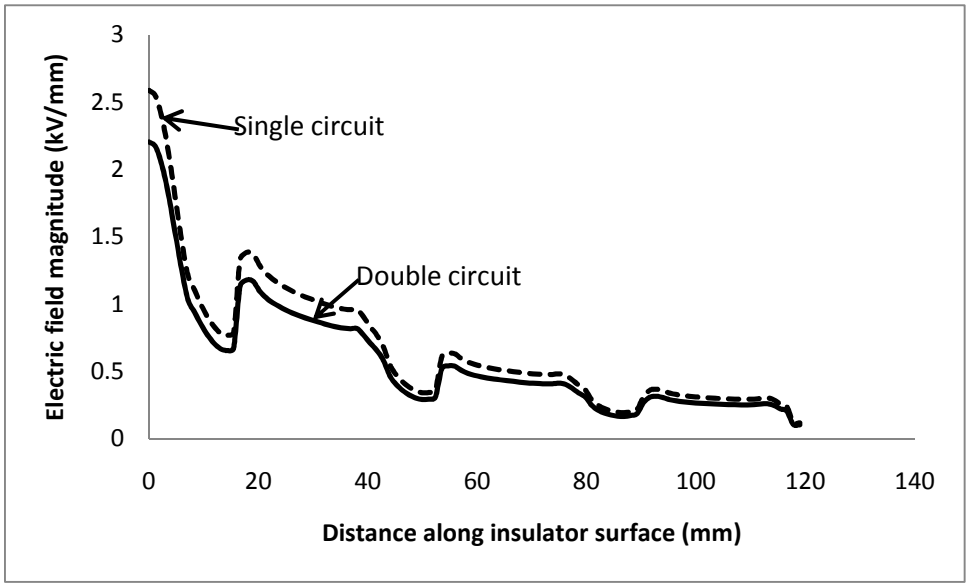

Figure 44. Electric field distribution along 230 kV single and double circuit dead end structures

6.7 Comparison between Simulations run in COULOMB and EPIC Software

Two sets of simulations are carried out to check the accuracy of the results obtained. This is done by carrying out the modeling in different environments, i.e. by using COULOMB and EPIC. Software. Although one is based on the concept of Boundary Element Method and the other on Charge Simulation Method, the electric field calculations carried out on both the platforms should be in good agreement.

6.7.1 Suspension Model for Voltage Rating 138 kV

138 kV suspension structure is modeled both in COULOMB and EPIC. The modeling carried out in EPIC is presented in section 6.2. This section focuses on the comparion between the results obtained by both the softwares. Each part of the geometry is constructed part by part with the dimesnions provided by EPRI Task Force on modeling Composite Insulators using the software COULOMB [6]. The entire model is contructed as the strucutre is not rotational symmetric. The specifications of the composite insulator modeled in COULOMB, shown in Figure 45, are the same as that used in EPIC. Table 6-10 compares the results obtained by both

the software. The electric field is measured along the five different location described in section 6.2.6.

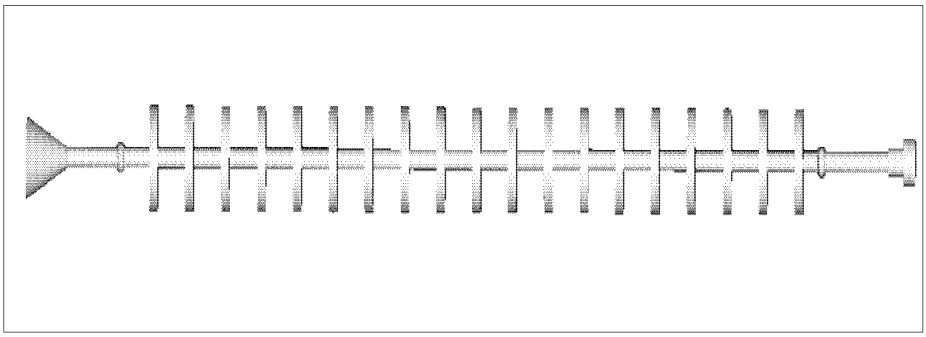

Figure 45. 138 kV suspension insulator modeled in COULOMB

Table 6-10 Comparison in results from EPIC and COULOMB for electric field along 138 kV suspension insulator

	Maximum electric field (kV/mm)				
	I.	II.	III.	IV.	V.
COULOMB	1.26	0.27	0.93	2.62	0.46
EPIC	1.32	0.36	0.78	2.13	0.55

It can be seen that the results do not match exactly but are in close provimity. Some differences arise due to the differetn concepts used by both the softwares and also the modeling techniques.

6.7.2 Effect of Bundled Conductors on Electric Field Calculations

Simulations are carried out in COULOMB and EPIC software for 500 kV suspension structure with single circuit. The number of conductors in the bundle is varied to analyze the electric field distribution along the composite insulators used. The specifications of the entire geometry, tower structure, phase and ground conductors, and hardware attachment structures are documented in Appendix D. The specifications of the composite insulator modeled in EPIC and COULOMB are presented in Table 6-11 and Table 6-12.

Table 6-11 Dimensions of 500 kV composite insulator modeled in EPIC

Manufacturer	Hubbell Power Systems
Insulator type	Hi*Lite
Catalog#	513028
SML	50 kip
Energized end fitting	Ball
Grounded end fitting	Eye
Base connection length	4676 mm
Leakage distance	10795 mm
Shed type	Regular
Number of sheds	112
Energized end corona ring diameter	15 inch
Grounded end corona ring diameter	15 inch

Table 6-12 Dimensions of 500 kV composite insulator modeled in COULOMB

Manufacturer	Xinjiang Energy
Catalog#	513028
Energized end fitting	Ball
Grounded end fitting	Eye
Base connection length	5000 mm
Leakage distance	13750 mm
Energized end corona ring diameter	15 inch
Grounded end corona ring diameter	15 inch
Relative permittivity Silicone	3
Relative permittivity Fiberglass rod	5
Relative permittivity Steel	1

Bundled conductors can be oriented in two different ways. i.e. with apex down or side down. Apex down means that the polygon formed by the bundled conductors is oriented with one vertex (or apex) at the bottom. Side down refers to the orientation where one of the sides of the polygon is placed horizontally at bottom, parallel with the ground base. For instance, for a bundled with six conductors, apex down and side down orientation is shown in Figure 48. For the purpose of this work, side down configuration is considered.

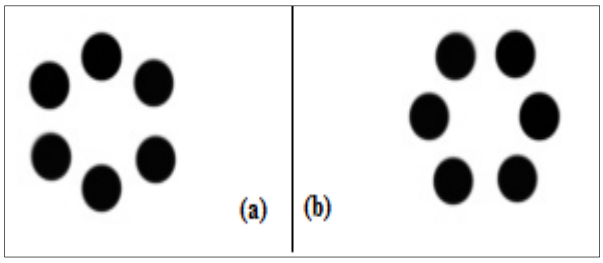

Figure 46. Bundled conductor orientations (a) Apex down (b) Side down

The number of conductors in one bundle are varied from one through six, the results obrained from both the softwares are presented in Table 6-13 for comparison purpose:

Table 6-13 Comparison in results from EPIC and COULOMB for electric field along 500 kV suspension insulator as a function of number of conductors in a bundle

Number of conductors in a bundle	6	4	3	2	1
	Maximum electric field (kV/mm)				
COULOMB	0.454	0.515	0.609	0.671	0.792
EPIC	0.42	0.465	0.543	0.590	0.721
Percentage difference	7 %	10%	11%	12%	9%

Comparisons made in the electric field distribution from results obtained by the two softwares do not show a large variance. Both the softwares have their own advantages. EPIC proves to be more efficient in terms of computation and modeling time when it comes to more complex models including the entire tower geometry of transmission structures. COULOMB exhibits excellent scope for customizing the model to any extent the user wishes to. Wet conditions can also be modeled in COULOMB.

7. CONCLUSIONS AND FUTURE WORK

7.1 Conclusion

This research was aimed at analysis of composite insulators used in transmission systems with the aid of numerical analysis techniques. This technique can be used to investigate the various factors that affect the electric field and voltage distribution along composite insulators without the need of performing physical laboratory experiments which could prove to be very expensive and exhaustive. This tool is extremely useful in designing EHV and UHV composite insulators. Various conclusions drawn from this research work are:

- Various numerical electric field analysis techniques were discussed in detail out of which two were chosen to carry out this work. Designing included establishing optimum number of boundary element conditions in order to obtain an accurate solution keeping the computation time in reasonable.
- The electric field calculations along composite insulators under dry conditions showed that the maximum electric field value depends on the system voltage. The field magnitude is greater for systems at higher voltages. The maximum field value was found to occur at the junction of the metallic energized end fitting-rubber housing-air.
- Comparison of the electric field magnitudes for composite insulators with porcelain (taken from literature) have shown the composite insulators witness higher electric stress when compared to porcelain.
- Field mitigating techniques like corona rings installed on composite insulators at different voltage ratings help in mitigating the electric field to appreciable levels. Corona rings are highly recommended even for lower system voltages (230 kV and 345 kV). For composite insulators used in UHV systems, an additional field mitigating device might be necessary.
- The effect of bundled conductors on the electric field distribution along composite insulators was analyzed. It was concluded that the maximum electric field reduces as the number of conductors in a bundle is increased. Considering the practical limitations on the number of

conductors per bundle, 4 for EHV systems and 6 for UHV systems are recommended based on acceptable E-field levels. Also, the effect of bundled conductors on the electric field along composite insulators was found to be more prominent for higher system voltages.

- Optimization was performed on a corona ring used for a 1000 kV composite insulator. The details for optimal parameters of the large corona ring were found to be: diameter of the ring, D= 1000 mm, thickness of the ring tube, T= 120 mm and projection from the energized end fitting, P= 400 mm.
- The use of large grading ring for designs employing double strings composite insulators not only showed an improved electric field and voltage distribution along the insulator but also reduced the maximum field value seen close to the junction between the energized end fitting and polymer surface. Also, the insulation distance, which bears 50% of the total applied voltage, is raised to be 1860 mm with the grading ring installed, while the distance without the grading ring is only 1150 mm in case of 1000 kV double string composite insulator, thereby making the voltage distribution more linear.
- Under wet conditions, the electric field spikes at the water-rubber housing-air junction and exceeds the streamer threshold value. The electric field enhancement is higher for composite insulators at higher voltages.
- Comparisons were made between composite insulators used in dead end and suspension environments for 138 kV rated system voltage. E-field analysis showed that the dead end insulators undergo as much as 11 % higher electric stress when compared to suspension.
- The same was repeated up to voltage level 500 kV and it was observed that the dead end composite insulators experience significantly higher electric stress when compared to composite suspension insulators. And this difference was found to get more prominent as the system voltage increases.
- Electric field calculations were made along composite insulators used in single dead end and double dead end environments. It was concluded that the composite insulators used in single

dead end structures experienced as much as 18 % higher electric stress when compared to the ones used in double dead end structures.

7.2 Future Work

- Electric field mitigation techniques used in wet conditions may be developed.
- The effect of water droplets on shed and sheath region of composite insulators may be investigated and the electric field value for corona inception may be established.
- The effects of multiple water droplets, their volume, angle of contact and water conductivity might be varied to study their effect on electric field magnitudes. These could help in performance analysis of composite insulators under wet conditions.

REFERENCES

[1] R. S. Gorur, E. A. Cherney and J. T. Burnham, *Outdoor Insulators*, Ravi S. Gorur Inc., phoenix, Arizona, USA, 1999.

[2] R. Lings, V. Chartier and P. S. Maruvada, "Overview of transmission lines above 700 kV," *IEEE PES Conference and Exposition* in Africa, pp. 33-43, 2005.

[3] A. J. Phillips, J. Kuffel, A. Baker, J. Burnham, A. Carreira, E. Cherney, W. Chisholm, M. Farzaneh, R. Gemignani, A. Gillespie, T. Grisham, R. Hill, T. Saha, B. Vancia, J. Yu, "Electric fields on AC composite transmission line insulators," *IEEE Transactions on Power Delivery*, v. 23, No. 2, pp. 823-830, 2008.

[4] J. S. T. Looms, *Insulators for High Voltage*, Peter Peregrinus Ltd, London, U. K., 1988.

[5] Anonymous, *Xinjiang New Energy Catalog*, China.

[6] Anonymous, EPRI Task Force on E-field modeling of composite insulators.

[7] Anonymous, Data from Salt River Project for a 230 kV system, Salt River Project.

[8] A. C. Baker, "Insulators 101 Section C – Standards," *IEEE PES Transmission and Distribution Conference and exposition*, pp. 1-5, April, 2010.

[9] Anonymous, *COULOMB 8.0 Users and Technical manual*, Integrated Engineering Software, Canada.

[10] K. Shenoi, R. S. Gorur, "Evaluation of station post insulator performance from electric field calculations," *IEEE Transaction on Dielectrics and Electrical Insulation*, v. 15, No. 6, pp. 1731-1738, December 2008.

[11] A. J. Phillips, D. J. Childs, H. M. Schneider, "Aging of non-ceramic insulators due to corona from water droplets," *IEEE Transactions on Power Delivery*, v. 14, No. 3, July 1999.

[12] N. L. Allen, A. Ghaffar, "The conditions required for the propagation of a cathode-directed positive streamer in air," *Journal of Physics D: Applied Physics*, v. 28, pp. 331-337, 1995.

[13] F. A. M. Rizk, "Mechanism of insulator flashover under artificial rain" *Proceeding of IEE*, v. 122, No. 4, pp. 449-454, April 1975.

[14] V. V. Dan, "A rational choice of bundle conductors configuration," *Proceedings of 1998 International Symposium of Electrical Insulating Materials*, pp. 349-354, September 1998.

[15] EPRI, *Transmission Line Reference Book*, 1975.

[16] Y. Shu, *China builds UHV Grid*, State Grid Corporation of China, pp. 80, March 2010.

[17] Anonymous, *Focus on UHV AC: China shows the way by energizing 1000 kV*, Global Transmission.

[18] D. Huang, J. ruan, Y. Chen, F. Huo, "Calculation and measurement of potential and electric field distribution along 1000 kV AC transmission line composite insulator," *International Conference on Electrical Machines and Systems*, pp. 428-433, October 2008.

[19] Anonymous, *Manual for EPIC software*, EPRI.

[20] IEEE Standard Dictionary of Electrical and Electronics Terms

[21] K. L. Chrzan, F. Moror, "Concentrated discharge and dry bands on polluted outdoor insulators," *IEEE Transactions on Power Delivery*, v. 22, No. 1, January 2007.

[22] R. S. Gorur, J. Chang, O. G. Amburgey, "Surface hydrophobicity of polymers used for outdoor insulation", *IEEE Transactions on Power Delivery*, v. 5, No. 4, pp. 1923-1933, October 1990.

[23] W. Que, S. S. Sebo, "Electric field and potential distribution along non-ceramic insulators with water droplets," *Electrical Insulation Conference and Electrical Manufacturing and Coil Winding Conference*, pp. 441-444, Cincinnati, Ohio, USA, October 2001.

[24] G. G. Karady, M. Shah, R. L. brown, "Flashover mechanism of silicone rubber insulators used for outdoor insulation – I," *IEEE Transactions on Power Delivery*, v. 10, No. 4, pp. 1965-1971, October 1995.

[25] R. T. Waters, R. E. Jones, "The impulse breakdown voltage and time lag characteristics of long gaps in air: The positive discharge", *Proceedings of the Royal Society of London Series A, Mathematical and Physical Sciences*, v. 256, No. 1069, pp. 185-212, April 1964.

[26] D. A. Swift, "Flashover of an insulator surface in air due to polluted water droplets," *Proceedings of the 4th International Conference on properties and Applications of Dielectric Materials*, July 3-8, 1994, Australia.

[27] Z. Guan, L. Wang, B. yang, X. Liang, "Electric field analysis of water droplet corona," *IEEE Transactions on Power Delivery*, v. 20, No. 2, pp. 964-969, April 2005.

[28] E. Kufel, W. S. Zaengel, *High Voltage Engineering Fundamentals*, Pergamon Press, 1988.

[29] P. B. Zou, *Numerical Analysis of Electromagnetic Fields*, Springer-Verlag, Berlin, 1993.

[30] G. Swift, T. S. Molinski, R. Bray, R. Menzies, “A fundamental approach to transformer thermal modeling - Part II: field verification,” *IEEE Transactions of Power Delivery*, v. 16, No. 2, Apr 2001, pp. 176-180.

[31] D. Susa, M. Lehtonen, H. Nordman, “Dynamic thermal modeling of power transformers,” *IEEE Transactions on Power Delivery*, v. 20, No. 1, Jan 2005, pp. 197-204.

[32] D. Susa, M. Lehtonen, “Dynamic thermal modeling of power transformers, further developments Part I,” *IEEE Transactions on Power Delivery*, v. 21, No. 4, Oct 2006, pp. 1961-1970.

[33] D. Susa, M. Lehtonen, “Dynamic thermal modeling of power transformers, further developments Part II,” *IEEE Transactions on Power Delivery*, v. 21, No. 4, Oct 2006, pp. 1971-1980.

[34] L. Jauregui-Rivera, D. J. Tylavsky, “Acceptability of four transformer top-oil thermal models-Part I: defining metrics,” *IEEE Transactions on Power Delivery*, v. 23, No. 2, Apr 2008, pp. 860-865.

[35] L. Jauregui-Rivera, D. J. Tylavsky, “Acceptability of four transformer top-oil thermal models-Part II: comparing metrics,” *IEEE Transactions on Power Delivery*, v. 23, No. 2, Apr 2008, pp. 866-872.

[36] D. J. Tylavsky, Q. He, G. A. McCulla, J. R. Hunt, “Sources of error in substation distribution transformer dynamic thermal modeling,” *IEEE Transactions on Power Delivery*, v. 15, No. 1, Jan 2000, pp. 178-185.

[37] Q. He, J. Si, D. J. Tylavsky, “Prediction of top-oil temperature for transformers using neural networks,” *IEEE Transactions on Power Delivery*, v. 15, No. 4, Oct 2000, pp. 1205-1211.

[38] D. J. Tylavsky, Q. He, J. Si, G. A. McCulla, J. R. Hunt, “Transformer top-oil temperature modeling and simulation,” *IEEE Transactions on Industry Applications*, v. 36, No. 5, Sept. – Oct. 2000, pp. 1219-1225.

[39] S. A. Ryder, Q. He, J. Si, D. J. Tylavsky, “Discussion of “Prediction of top-oil temperature for transformers using neural networks” and closure,” *IEEE Transactions on Power Delivery*, v. 16, No. 4, Oct 2001, pp. 825-826.

[40] D. J. Tylavsky, X. Mao, G. A. McCulla, “Transformer thermal modeling: improving reliability using data quality control,” *IEEE Transactions on Power Delivery*, v. 21, No. 3, Jul 2006, pp. 1357-1366.

APPENDIX A

138 KV SUSPENSION MODEL DATA

1) Specifications for Clamp (L2)

- Catalog # HAS -139-S
- Strength: 25000 lbs/11340 kg
- Length :8-7/8 inch/225.43 mm
- Width: 1-17/32 inch /38.89 mm
- Height: 3 inch/76.2 mm
- J: ½ inch/12.7 mm
- PD: 5/8 inch/15.88 mm
- Max Angle: 22.5
- Clamping range:0.90 – 1.39 inch/22.86 – 35.31 mm

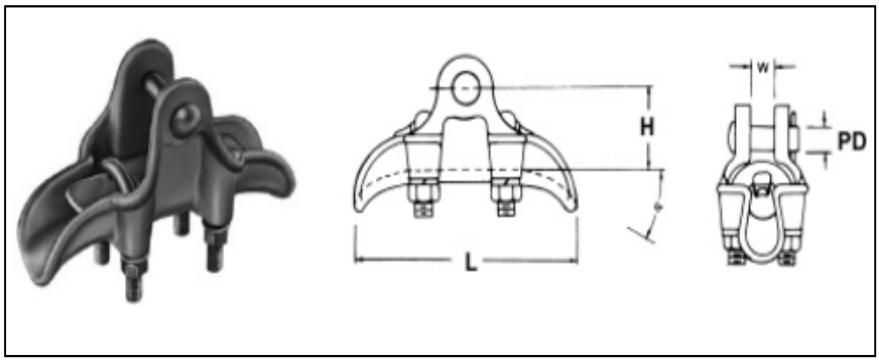

Figure 47. Clamp specifications used in 138 kV suspension configuration in EPIC

2) Link to Polymer (L5)

- Catalog # SA-13
- Strength:30000 lbs/13608 kg
- Length:2-1/16 inch/52.39 mm
- Width: 1-3/8 inch/ 34.93 mm
- Diameter: 11/16 inch / 17.46 mm
- R: 13/16 inch/ 20.64 mm

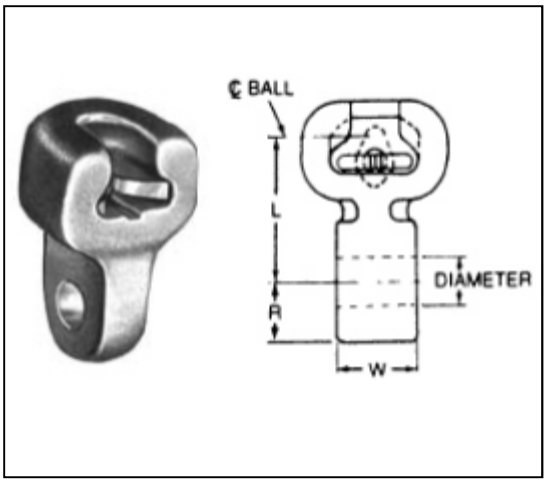

Figure 48. Link to polymer specifications used in 138 kV suspension configuration in EPIC

3) Polymer specifications

- Hubbel Power Systems
- Dry arc distance: 1316 mm
- Leakage distance: 2806 mm
- Insulator Type: Hi*Lite
- Standard Mechanical Load (SML): 25/30 KIP
- Number of Sheds: 28

4) Structure Attachment Hardware (SAH)

- Catalog # SAH-P-Custom-3
- L8: 4.375 inch/ 111.125 mm
- A: 2-3/4 inch / 69.85 mm
- B: 2-3/4 inch / 69.85 mm
- W: ¾ inch / 19.05 mm

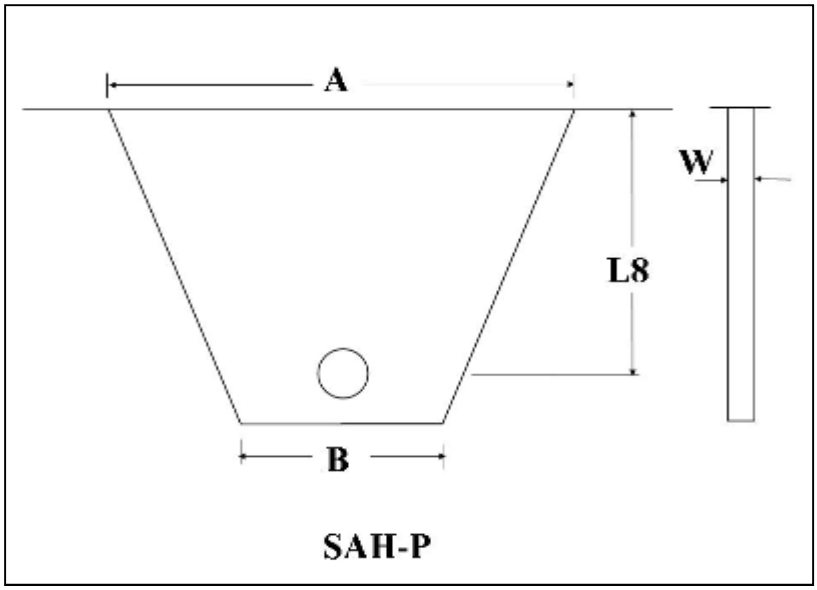

Figure 49. Structure attachment hardware specifications used in 138 kV suspension configuration in EPIC

APPENDIX B

138 KV DEAD END MODEL DATA

1) L1 SAH

- SAHD-HP-Custom 2
- L8: 4.375 inch/ 111.125 mm
- A:2-3/4 inch/69.85 mm
- B:2-3/4 inch /69.85 mm
- W: ¾ inch/19.05 mm

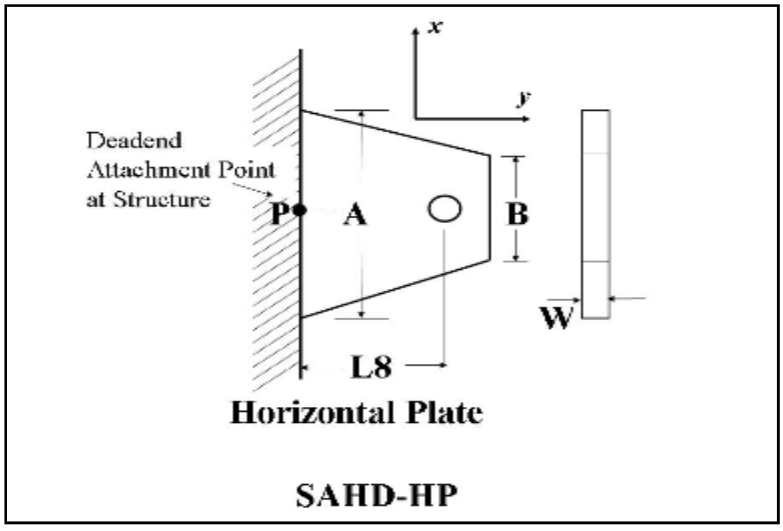

Figure 50. Structure attachment hardware specifications used in 138 kV dead end configuration in EPIC

2) L6 EPLink

- SYCS-30-90
- Strength: 30000lbs/13608 kg
- L: 2-9/32 inch /57.94 mm
- B: 1-3/16 inch/30.16 mm

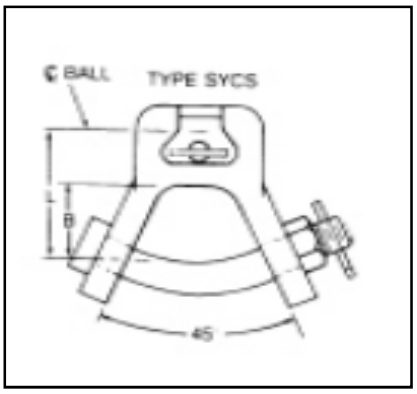

Figure 51. EP Link specifications used in 138 kV dead end configuration in EPIC

3) L 11 Dead End Connector: compression dead end type (CDE)

- # A0311
- Eye Orientation: horizontal
- Clamping range: 0.883-1.04 inch/ 22.4-26.4 mm
- L: 16.3 inch/413 mm
- A: 2 inch/ 50 mm
- B: 1inch/ 25 mm
- C: 0.6 inch/ 15 mm
- F:3 inch/ 76 mm
- DS: 1.1 inch/ 27.94 mm
- Number of bolts # 4
- BD: 1.75 inch/ 44 mm

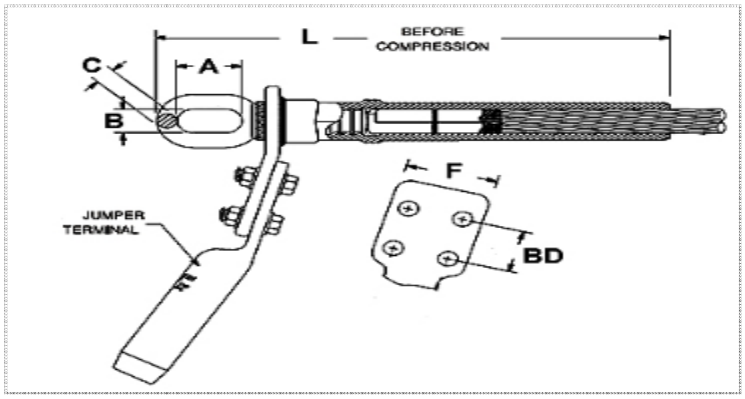

Figure 52. Dead end connector specifications used in 138 kV dead end configuration in EPIC

APPENDIX C

SPECIFICATION FOR 230 KV SINGLE AND DOUBLE DEAD END STRUCTURES

1) 230 kV Single Dead end Structure:

- Tower configuration: Tubular or Pole
- Catalog # STSIEEE

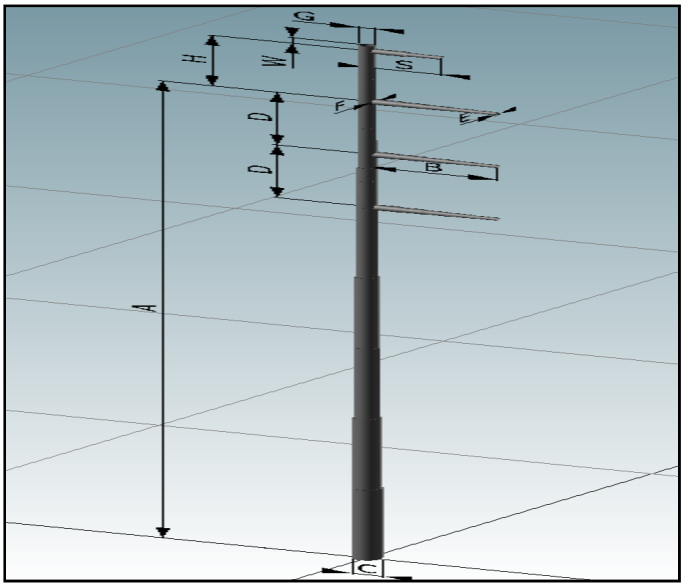

Figure 53. Schematic of single dead end tower structure for a 230 kV system in EPIC

Table C-1 Dimensions of single dead end tower structure used for 230 kV structure

	Dimensions (m)
A	27.15
B	2.65
C	0.6
D	3.13
E	0.14
F	0.31
G	0.30
H	3.00
S	1.50
W	0.33

2) Conductor specifications

- Phase conductor diameter: 2.81 mm
- Ground conductor diameter: 1.1 mm